

Supporting Information

Efficient screening rooted in a series of transition-metal atom anchored conjugated organic frameworks toward multifunctional HER/OER/ORR via modification of chalcogen ligands: a machine learning and constant potential study

Xiaomeng Cui^a, Yuanrui Li^a, Qiang Zhang^{*a}, Xihang Zhang^a, Weiju Hao^b, Yuling Song^c

Renxian Qin^a and Yali Lu^a

^a Department of Physics, College of Science, University of Shanghai for Science and Technology,
Shanghai 200093, People's Republic of China

^b School of Materials and Chemistry, University of Shanghai for Science and Technology,
Shanghai 200093, People's Republic of China

^c College of Physics and Electronic Engineering, Nanyang Normal University, Nanyang 473061,
People's Republic of China

* Corresponding author.

*Address correspondence to E-mail: qiangzhang@usst.edu.cn

Note S1. Calculation details of the binding energy (E_b).

To investigate the stabilities of candidates, the binding energy (E_b) of transition metal (TM) atoms embedded in the substrates is defined by the following equation:

$$E_b = E_{\text{TM-Sub}} - E_{\text{TM}} - E_{\text{Sub}} \quad (\text{S1})$$

where $E_{\text{TM-Sub}}$ represents the total energy of TM@C₁₅N₆XY₂H₅ monolayers. E_{TM} and E_{Sub} denote the energies of an isolated TM atom and the substrate, respectively.

Note S2. HER Processes in an Acidic Environment.

The complete processes for the Hydrogen Evolution Reaction (HER), in an acidic environment can be described by the following reactions:



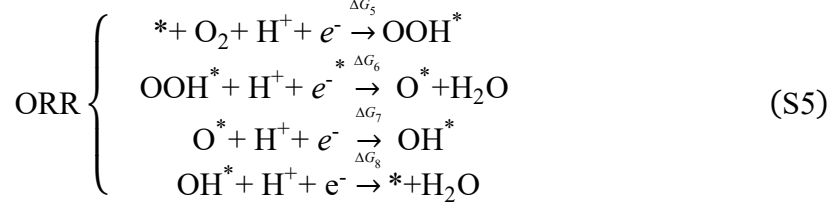
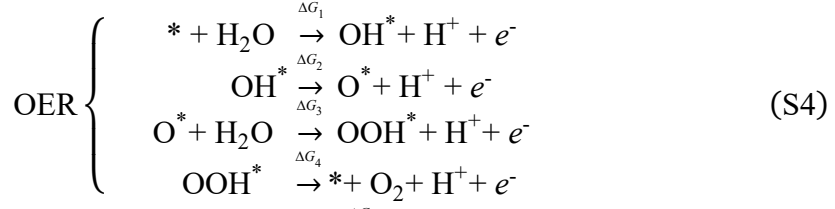
The Gibbs free energy of H* can be presented as:

$$\Delta G_{\text{H}^*} = \Delta E_{\text{H}^*} + \Delta E_{\text{ZPE}} + T\Delta S_{\text{H}^*} + \Delta G_{\text{pH}} + \Delta G_{\text{U}} \quad (\text{S3})$$

where ΔE is the total energy change. ΔE_{ZPE} is the zero-point energy correction. $T\Delta S$ is the entropy contribution. ΔG_{pH} is the free energy correction due to pH. ΔG_{U} is the free energy correction due to the applied electrode potential.¹

Note S3. OER, and ORR Processes in an Acidic Environment.

The complete processes for the Oxygen Evolution Reaction (OER), and Oxygen Reduction Reaction (ORR) in an acidic environment can be described by the following reactions:



where * is the substrate. The changes of Gibbs free energy in the above four OER/ORR processes can be described as $\Delta G_1 = -\Delta G_8 = G_{\text{OH}^*}$, $\Delta G_2 = -\Delta G_7 = G_{\text{OH}^*} - G_{\text{O}^*}$, $\Delta G_3 = -\Delta G_6 = G_{\text{OOH}^*} - G_{\text{O}^*}$ and $\Delta G_4 = -\Delta G_5 = 4.92 - G_{\text{OOH}^*}$. And the ΔG of each step can be presented as following:

$$\Delta G = \Delta E + \Delta E_{\text{ZPE}} + T\Delta S + \Delta G_{\text{pH}} + \Delta G_{\text{U}} \quad (\text{S6})$$

where ΔE is the total energy change. ΔE_{ZPE} is the zero-point energy correction. $T\Delta S$ is the entropy contribution. ΔG_{pH} is the free energy correction due to pH. ΔG_{U} is the free energy correction due to the applied electrode potential.²

Note S4. Overpotentials of HER, OER and ORR.

The overpotential values (η) can then be derived using equations provided:

$$\eta^{\text{HER}} = |\Delta G_{\text{H}^*}| \quad (\text{S7})$$

$$\eta^{\text{OER}} = \frac{\max \{\Delta G_1, \Delta G_2, \Delta G_3, \Delta G_4\}}{e} - 1.23 \text{ V} \quad (\text{S8})$$

$$\eta^{\text{ORR}} = 1.23 \text{ V} - \frac{\min \{\Delta G_1, \Delta G_2, \Delta G_3, \Delta G_4\}}{e} \quad (\text{S9})$$

Note S5. The hypothesis of exchange current.

The hypothesis of exchange current (i_0) proposed by Nørskov was used to describe The HER activity, which is defined as: $i_0 = -ek_0 \frac{1}{1 + \exp(\frac{|\Delta G_{\text{H}^*}|}{kT})}$, where k_0 is a rate constant,

typically used to describe the base value of the reaction rate. T is the absolute temperature, usually measured in Kelvin (K). k is the Boltzmann constant.

Note S6. Computational Method of the GBR Regression Algorithm

The Gradient Boosted Regression (GBR) model is an integrated machine learning algorithm composed of weak regression trees.^{3, 4} Given training samples $D = \{(x_1, y_1), (x_2, y_2), \dots, (x_n, y_n)\}$, with each regression tree having J leaf nodes, the input data is divided into J disjoint regions, and each regression tree is denoted as $t_m(x)$. The goal of GBR training is to minimize the loss function L , with the parameters θ_m determined by empirical risk minimization:

$$\theta_m = \underset{\theta_m}{\operatorname{argmin}} \sum_{i=1}^n L(y_i, f_{(m-1)}(x_i) + t_m(x_i)) \quad (\text{S10})$$

The GBR training process includes: (a) Initializing the regression tree function $f_0(x)$. (b) Training GBR using gradient descent and calculating the negative gradient of the loss function as the residual estimate. In the m^{th} iteration, GBR generates a regression tree based on the residuals and updates the function $f_m(x)$. (c) The final regression model is the weighted sum of multiple weak regression trees, expressed as:

$$f_M(x) = \sum_{m=1}^M t_m(x, \theta_m) \quad (\text{S11})$$

Note S7. Computational Method of the RFR Regression Algorithm

The Random Forest Regression (RFR) model is an ensemble learning technique used for regression.⁵ It constructs multiple decision trees during training and outputs the mean prediction of these trees. This method helps to alleviate the overfitting

problem often associated with individual decision trees. The RFR training algorithm utilizes bootstrap aggregating, or bagging, to create an ensemble of trees.

Given a training set $X = \{x_1, x_2, \dots, x_n\}$ with corresponding responses $Y = \{y_1, y_2, \dots, y_n\}$, bagging repeatedly (B times) selects random samples with replacement from the training set and fits trees to these samples:

For $b=1, \dots, B$: (a) Randomly sample n training examples from X, Y with replacement; call these samples X_b, Y_b . (b) Train a regression tree f_b on X_b, Y_b . After training, predictions for new samples x' are made by averaging the predictions from all the individual regression trees:

$$\hat{f} = \frac{1}{B} \sum_{b=1}^B f_b(x') \quad (\text{S12})$$

Note S8. Computational Method of the SVR Regression Algorithm

The Support Vector Regression (SVR) model is a supervised learning technique that employs algorithms for regression analysis.⁶ Given a training dataset with target values, SVR constructs a model to make predictions for new data points. SVR projects the training data into a high-dimensional space and seeks a hyperplane that best fits the data within a margin of tolerance ε .

The process of training an SVR model involves: (a) Minimizing $\frac{1}{2} \|w\|^2$. (b) Ensuring that $|y_i - \langle w, x_i \rangle - b| \leq \varepsilon$. where x_i represents a training sample and y_i is the corresponding target value. The term $\langle w, x_i \rangle - b$ denotes the predicted value for the sample, and ε defines the allowable margin of error. To handle cases where the constraints cannot be strictly satisfied, slack variables are introduced, allowing for a degree of approximation.

Note S9. Computational Method of the KNR Regression Algorithm

The K-Neighbour Regression (KNR) model, formulated by Thomas Cover, is a versatile non-parametric approach used for both regression and classification tasks⁶. In this method, the k nearest training samples in the feature space are identified. For regression purposes, the output is the mean of the property values of these nearest neighbors.

During the classification phase, the constant k is specified by the user. An unlabeled point (query or test sample) is classified by assigning it the most frequent label among the k closest training samples. Euclidean distance is commonly used for continuous variables, while metrics like the overlap metric or Hamming distance are suitable for discrete variables. The performance of k-NN classification can be significantly enhanced by optimizing the distance metric using algorithms such as Large Margin Nearest Neighbor or Neighborhood Components Analysis.

The KNR algorithm follows these steps: (a) Determine the Euclidean or Mahalanobis distance between the query sample and the labeled samples. (b) Arrange the labeled samples in order of increasing distance. (c) Select the optimal number k of nearest neighbors by minimizing the root mean square error (RMSE) through cross-validation. (d) Calculate the weighted average of the K nearest neighbors, inversely proportional to their distance.

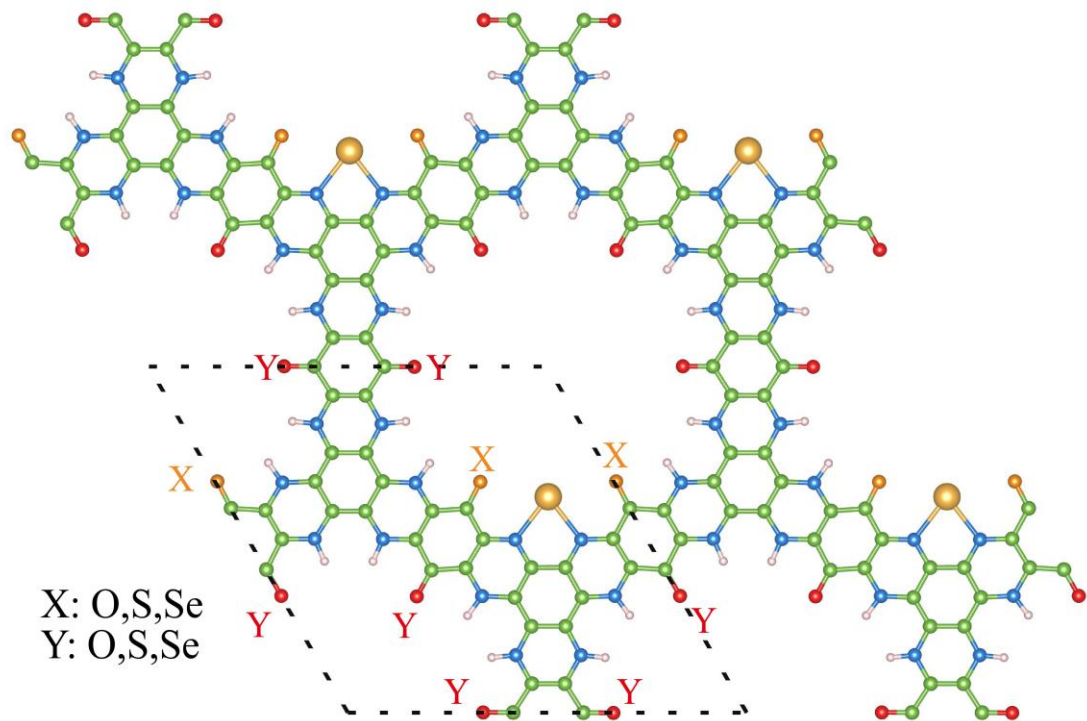


Fig. S1. Top view of the atomic structure of the $TM@C_{15}N_6XY_2H_5$ monolayer. The two kinds of chalcogen atoms were remarked respectively (X in brown, Y in red).

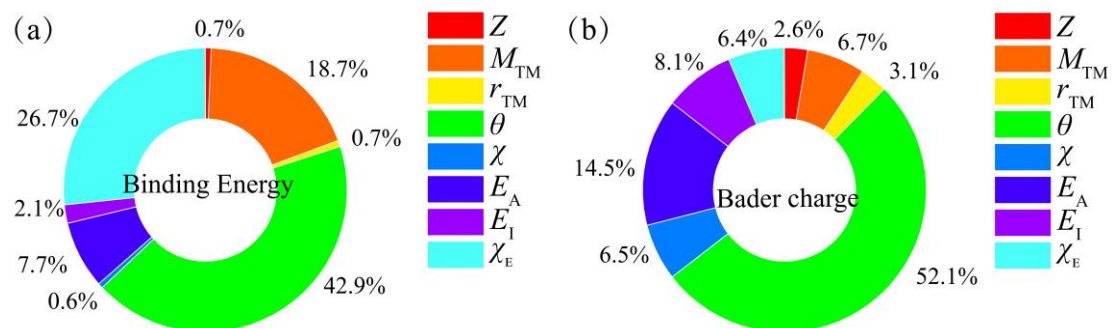


Fig. S2. The feature importance was predicted by the GBR and RFR algorithms for binding energies (a) and Charge transfer (b), respectively.

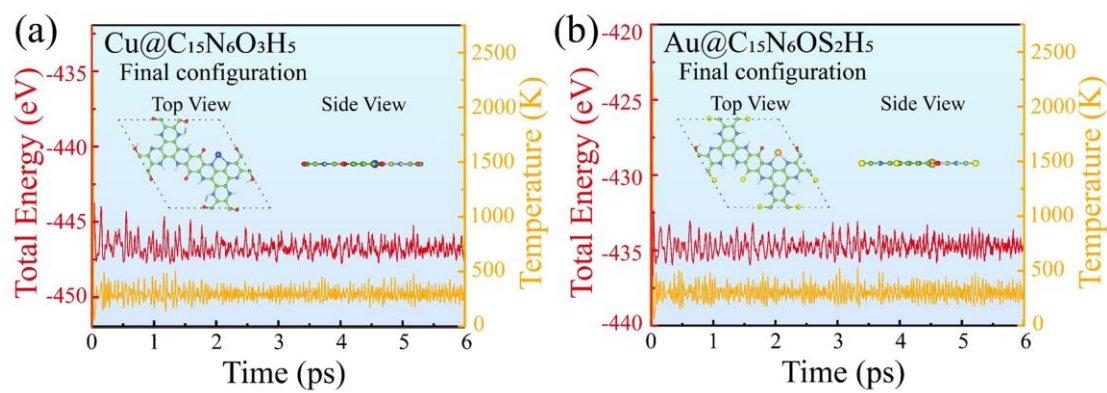


Fig. S3. AIMD simulations and snapshots of the final frame of the Cu@C₁₅N₆O₃H₅ (a) and Au@C₁₅N₆OS₂H₅ (b) monolayers at 300 K lasting 6 ps.

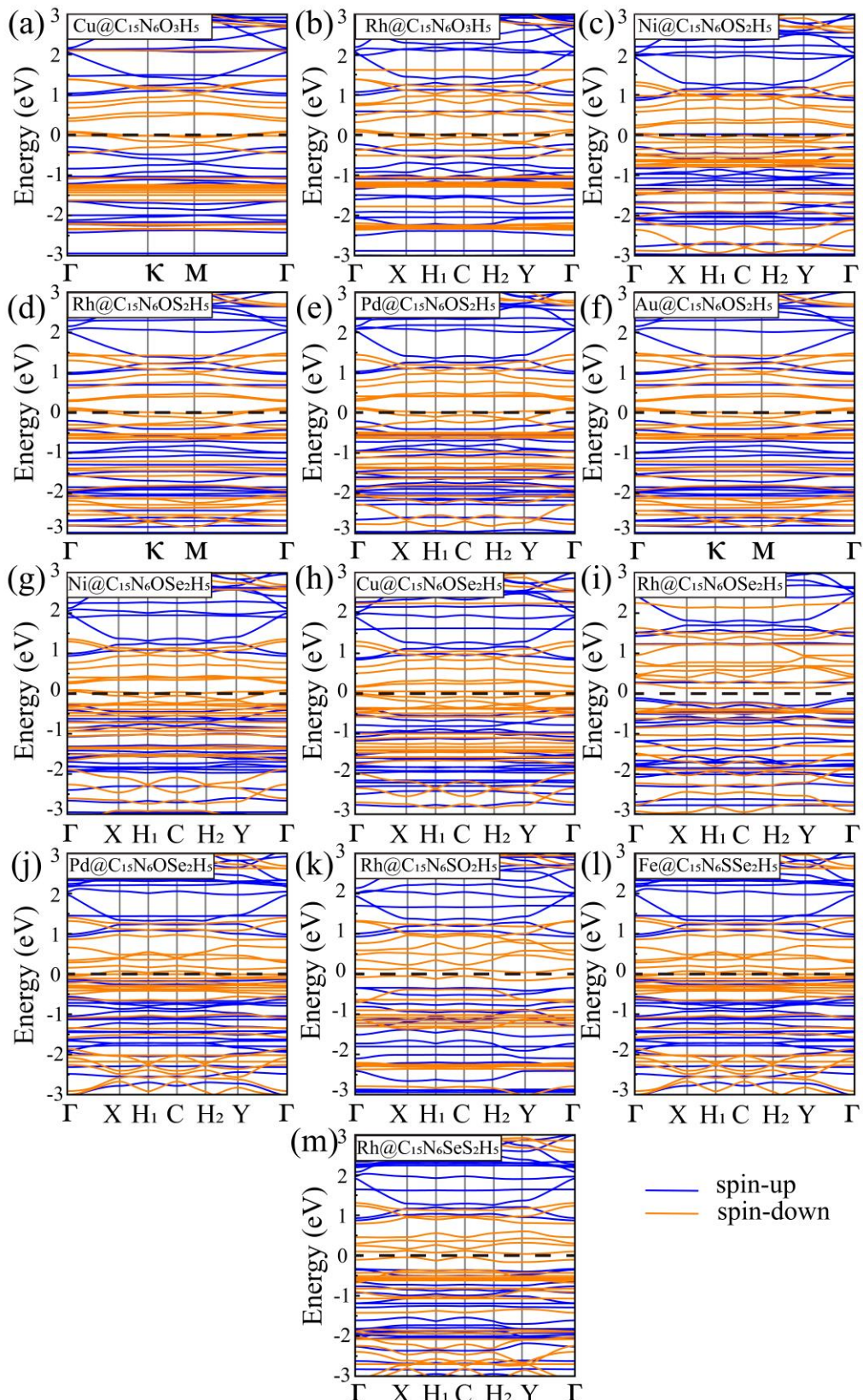


Fig. S4. Spin-polarized band structures of the selected TM@C₁₅N₆XY₂H₅ monolayers

with high activity, where the Fermi level is set as zero.

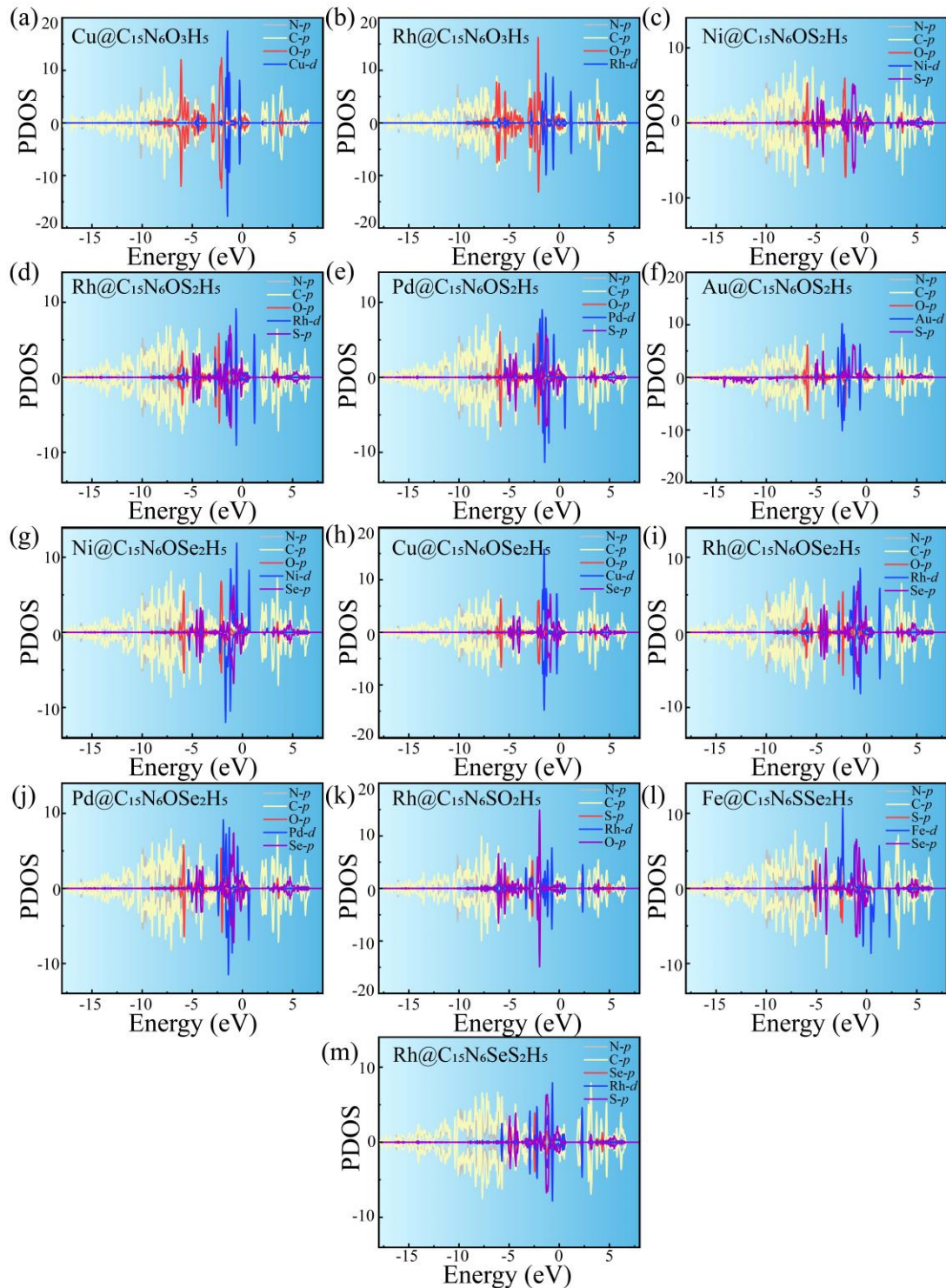


Fig. S5. Density of states of the selected TM@C₁₅N₆XY₂H₅ monolayers with high activity, where the Fermi level is set as zero.

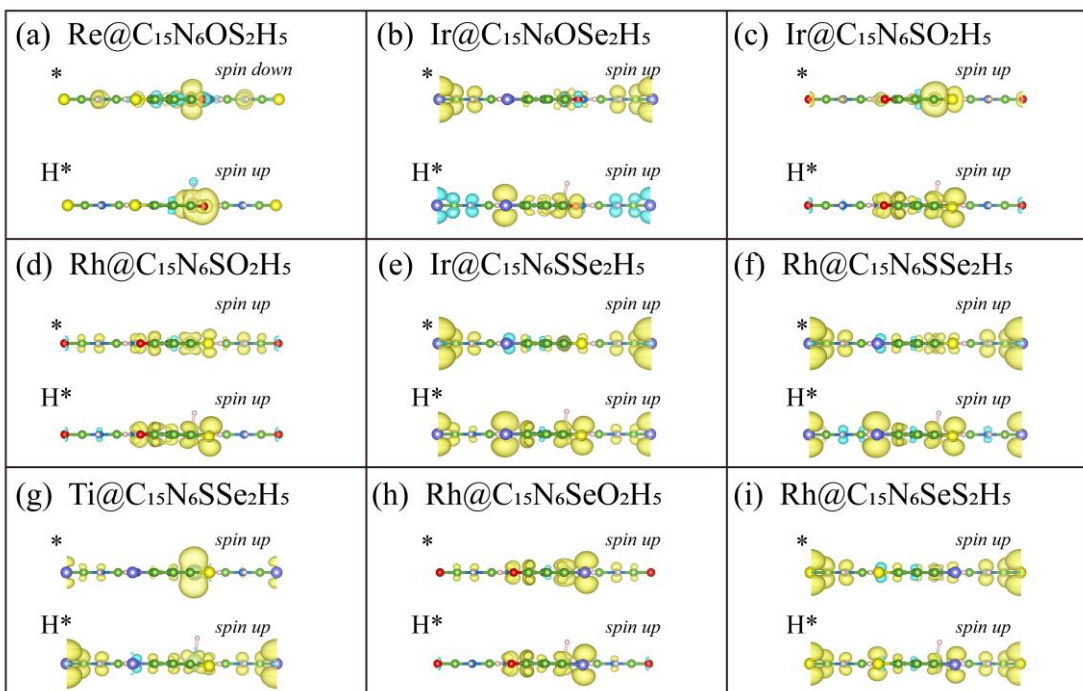


Fig. S6. The screened TM@C₁₅N₆XY₂H₅ monolayers' spin charge density for * and H*, where yellow represents spin up and blue represents spin down.

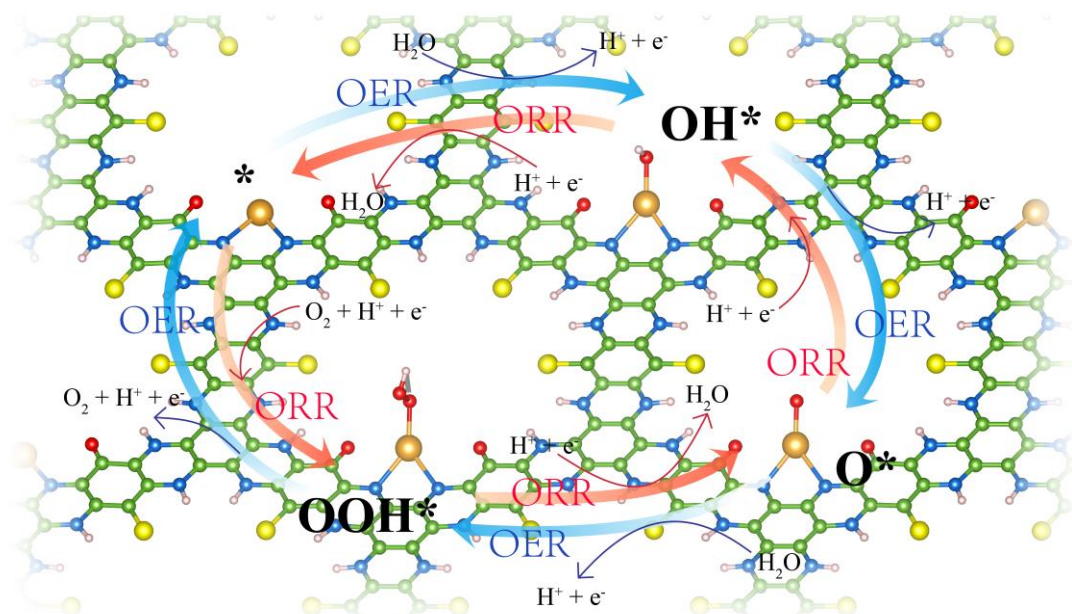


Fig. S7. Schematic diagram of OER/ORR on TM@C₁₅N₆XY₂H₅.

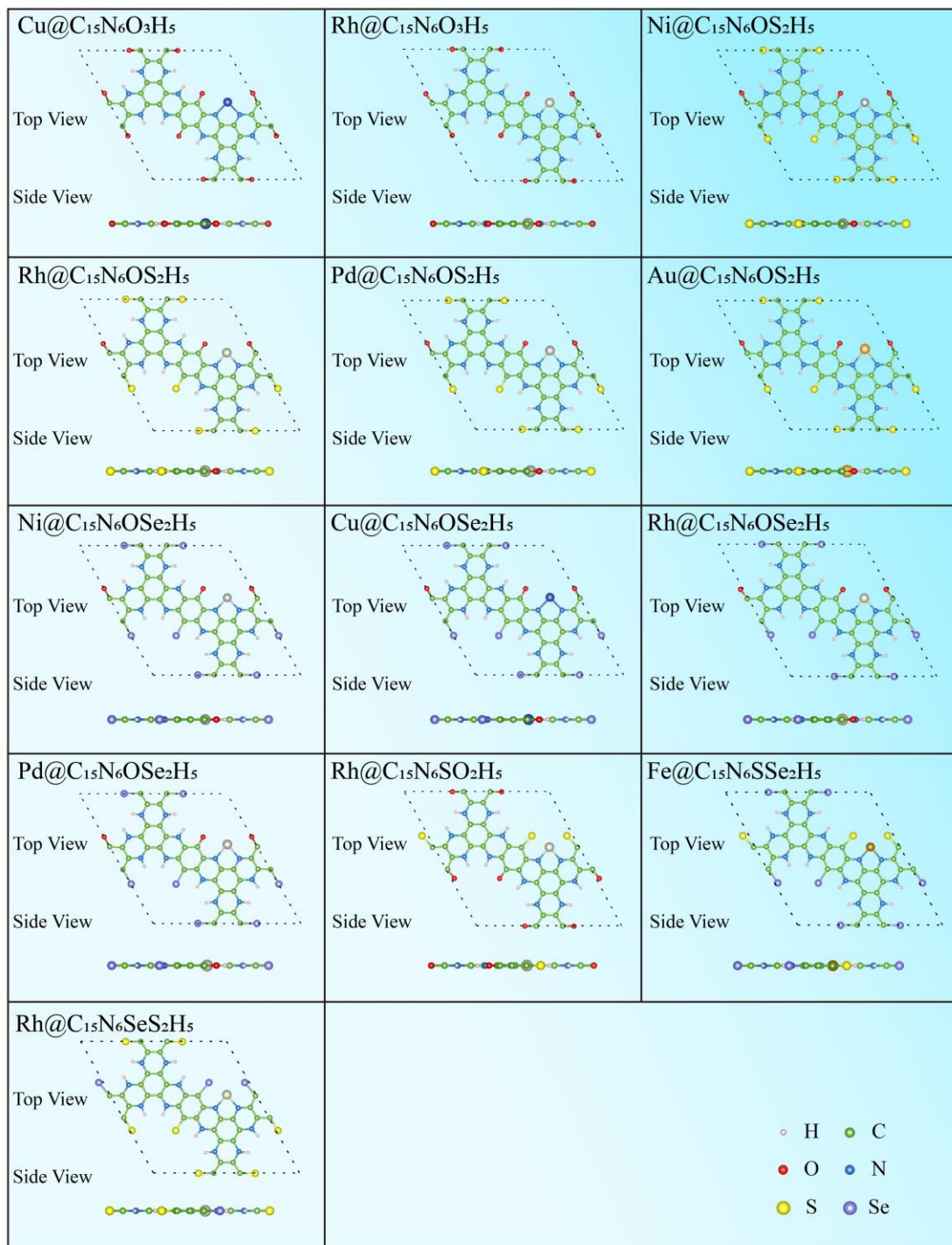


Fig. S8. The atomic motifs with high activity for bare TM@C₁₅N₆XY₂H₅ slab.

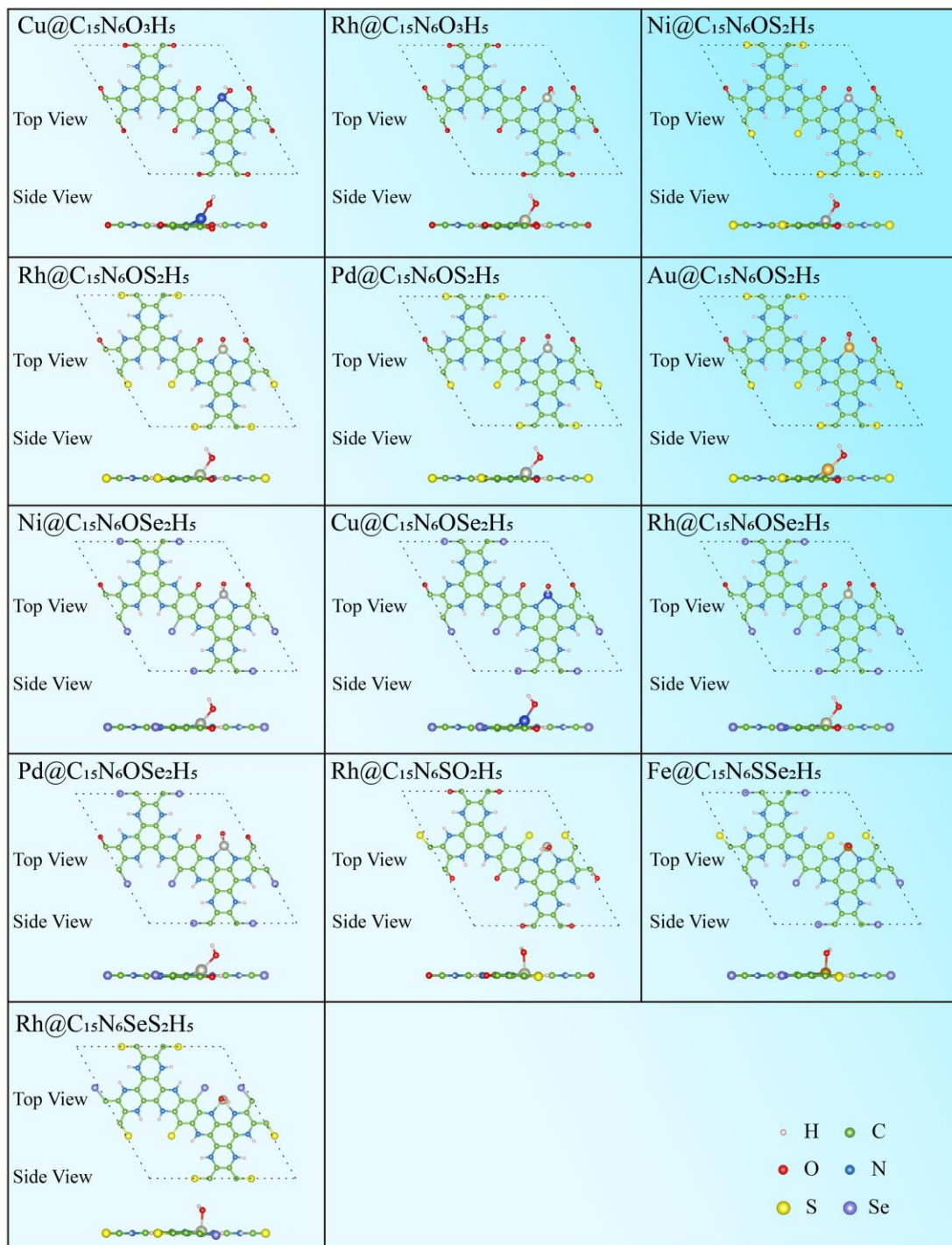


Fig. S9. The atomic motifs with high activity for OH adsorbed TM@C₁₅N₆XY₂H₅ monolayers.

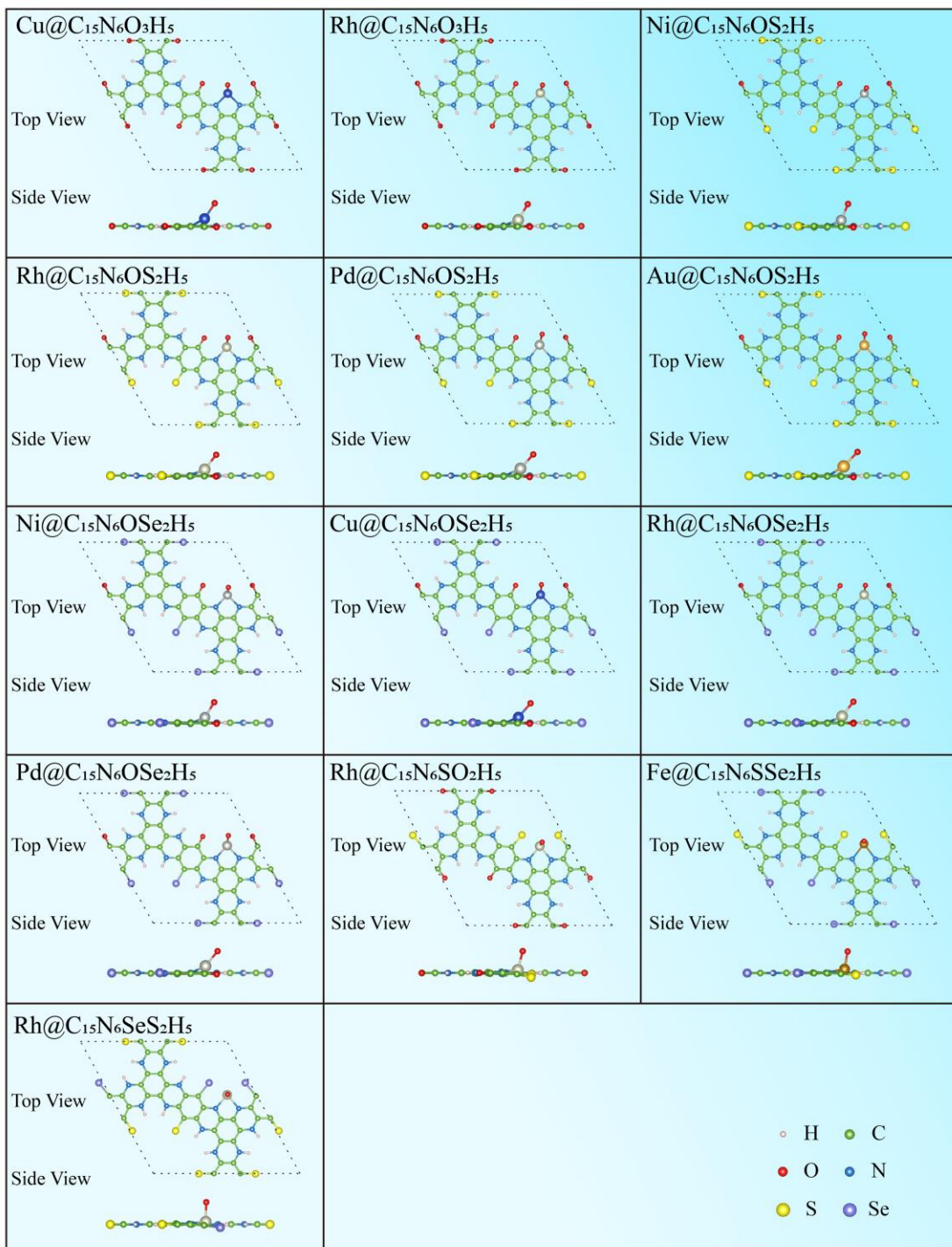


Fig. S10. The atomic motifs with high activity for O adsorbed TM@C₁₅N₆XY₂H₅ monolayers.

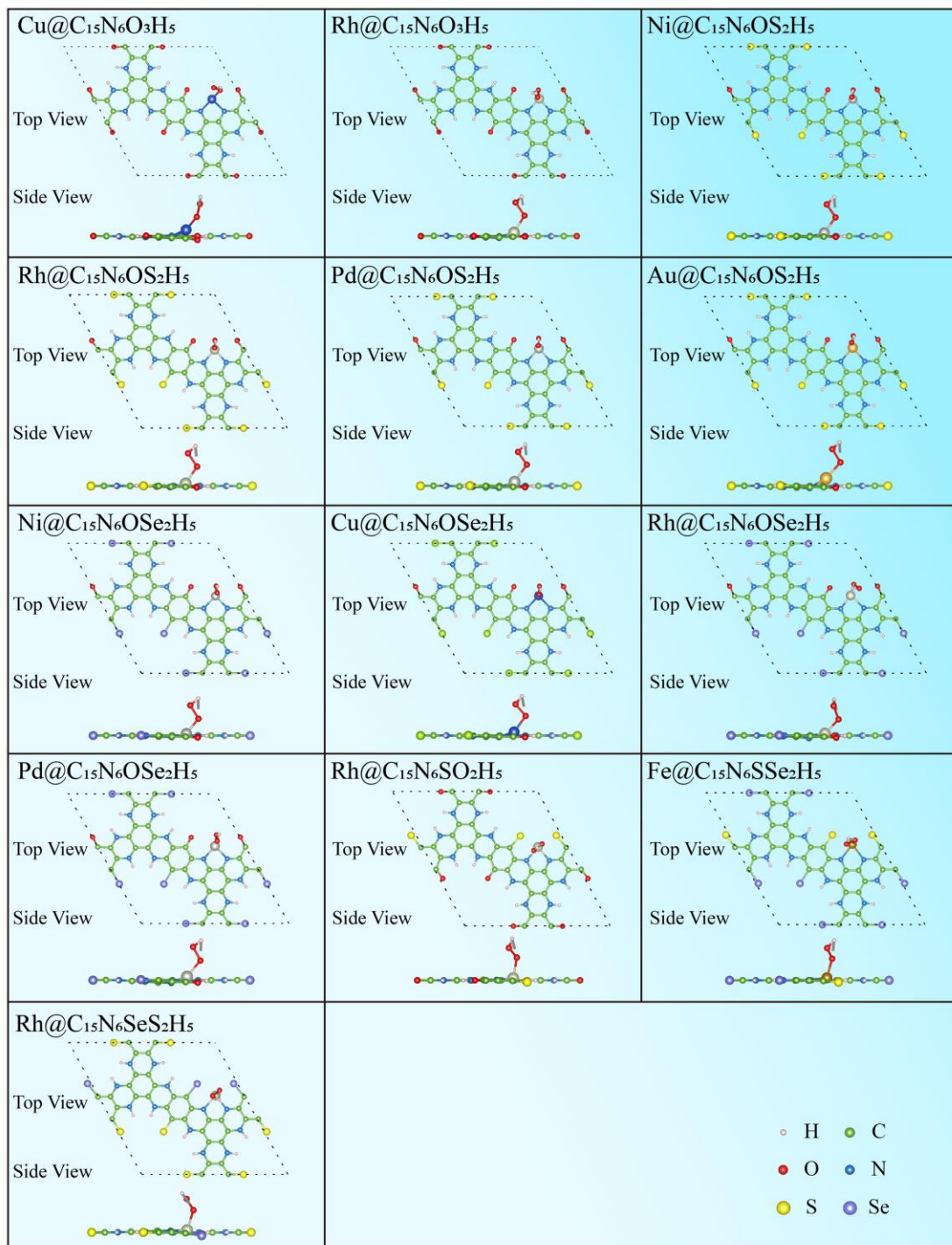


Fig. S11. The atomic motifs with high activity for OOH adsorbed TM@C₁₅N₆XY₂H₅ monolayers.

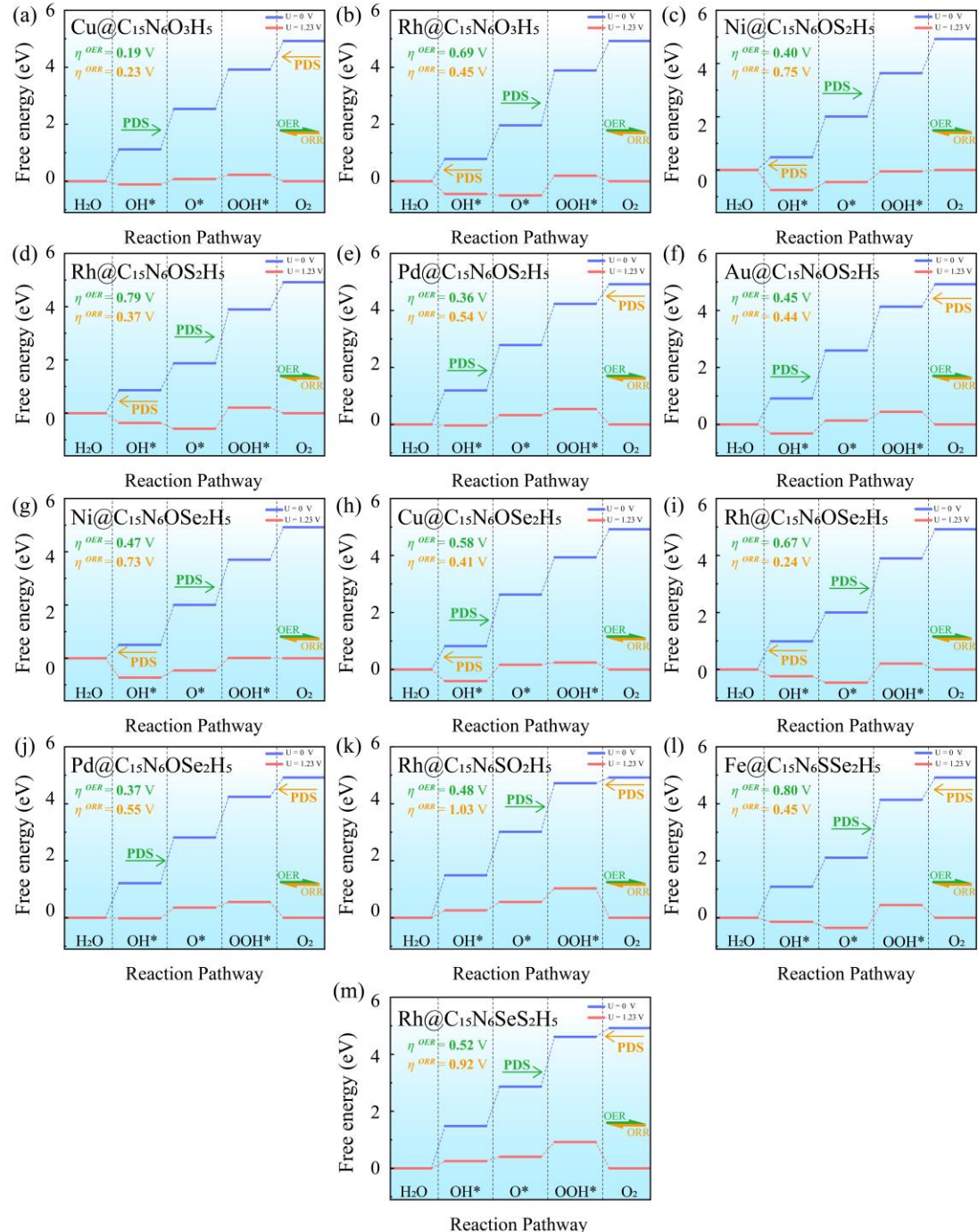


Fig. S12. The screened TM@C₁₅N₆XY₂H₅ monolayers' Gibbs free energy diagrams

including the OER and ORR processes

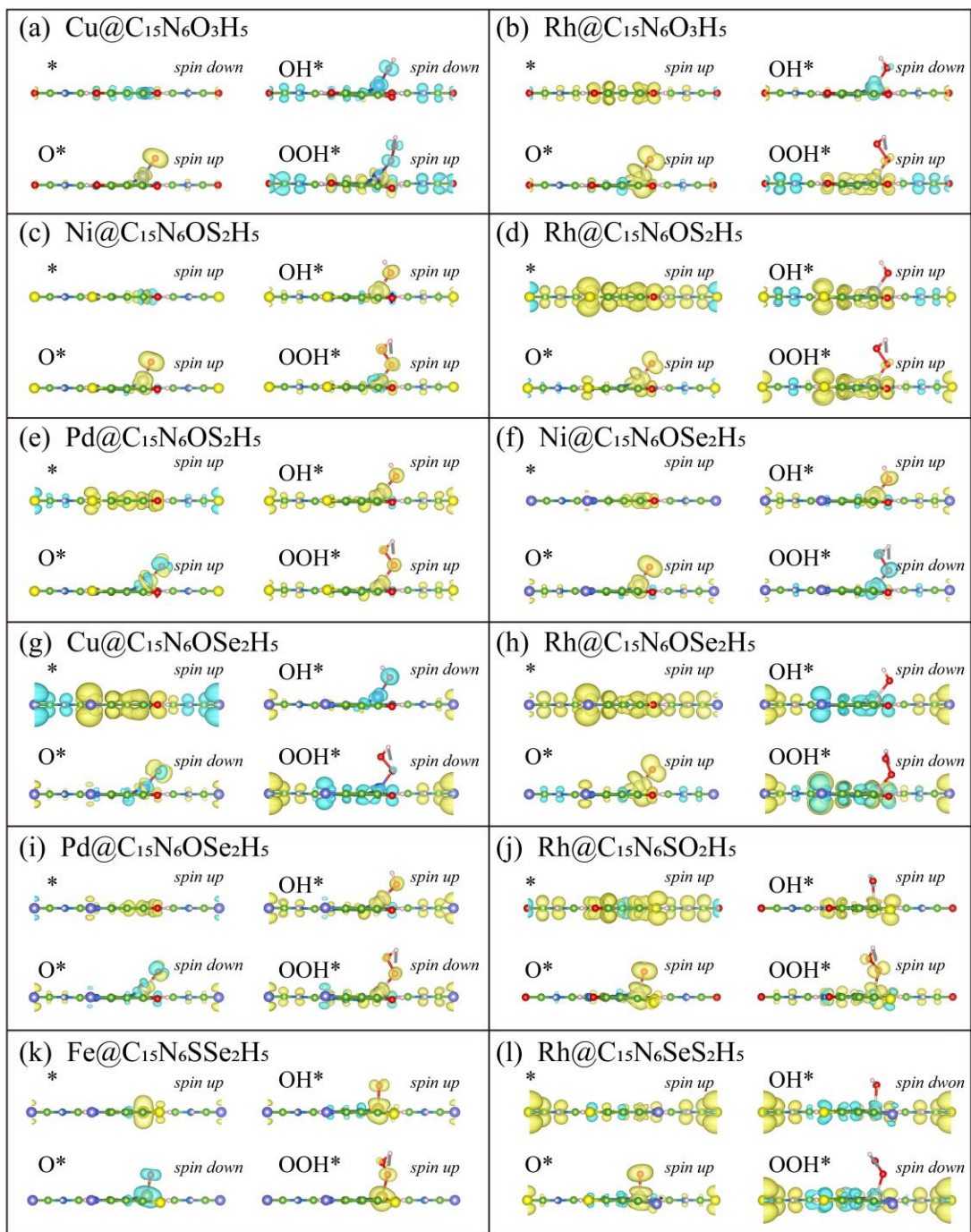


Fig. S13. The screened TM@C₁₅N₆XY₂H₅ monolayers' spin charge density for *, OH*, O*and OOH*, where yellow represents spin up and blue represents spin down.

Au@C₁₅N₆OS₂H₅

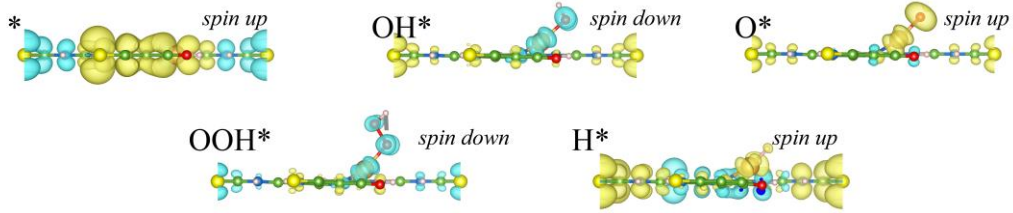


Fig. S14. The Au@C₁₅N₆OS₂H₅'s spin charge density for *, H*, OH*, O*and OOH*,

where yellow represents spin up and blue represents spin down

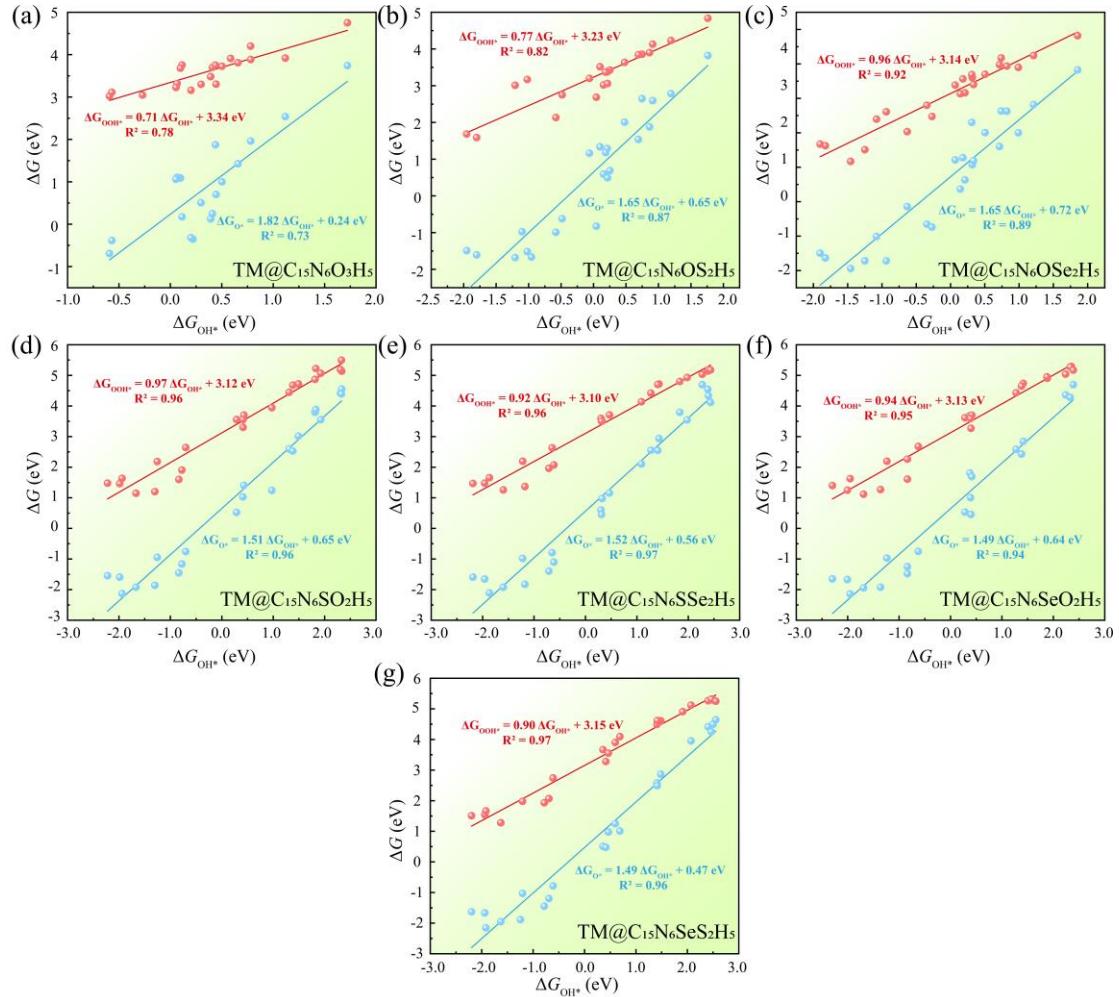


Fig. S15. Scaling relationships between ΔG_{OOH^*} and ΔG_{OH^*} (red), ΔG_{O^*} and ΔG_{OH^*} (blue) for (a) TM@C₁₅N₆O₃H₅, (b) TM@C₁₅N₆OS₂H₅, (c) TM@C₁₅N₆OSe₂H₅, (d) TM@C₁₅N₆SO₂H₅, (e) TM@C₁₅N₆SSe₂H₅, (f) TM@C₁₅N₆SeO₂H₅, and (g) TM@C₁₅N₆SeS₂H₅ monolayers.

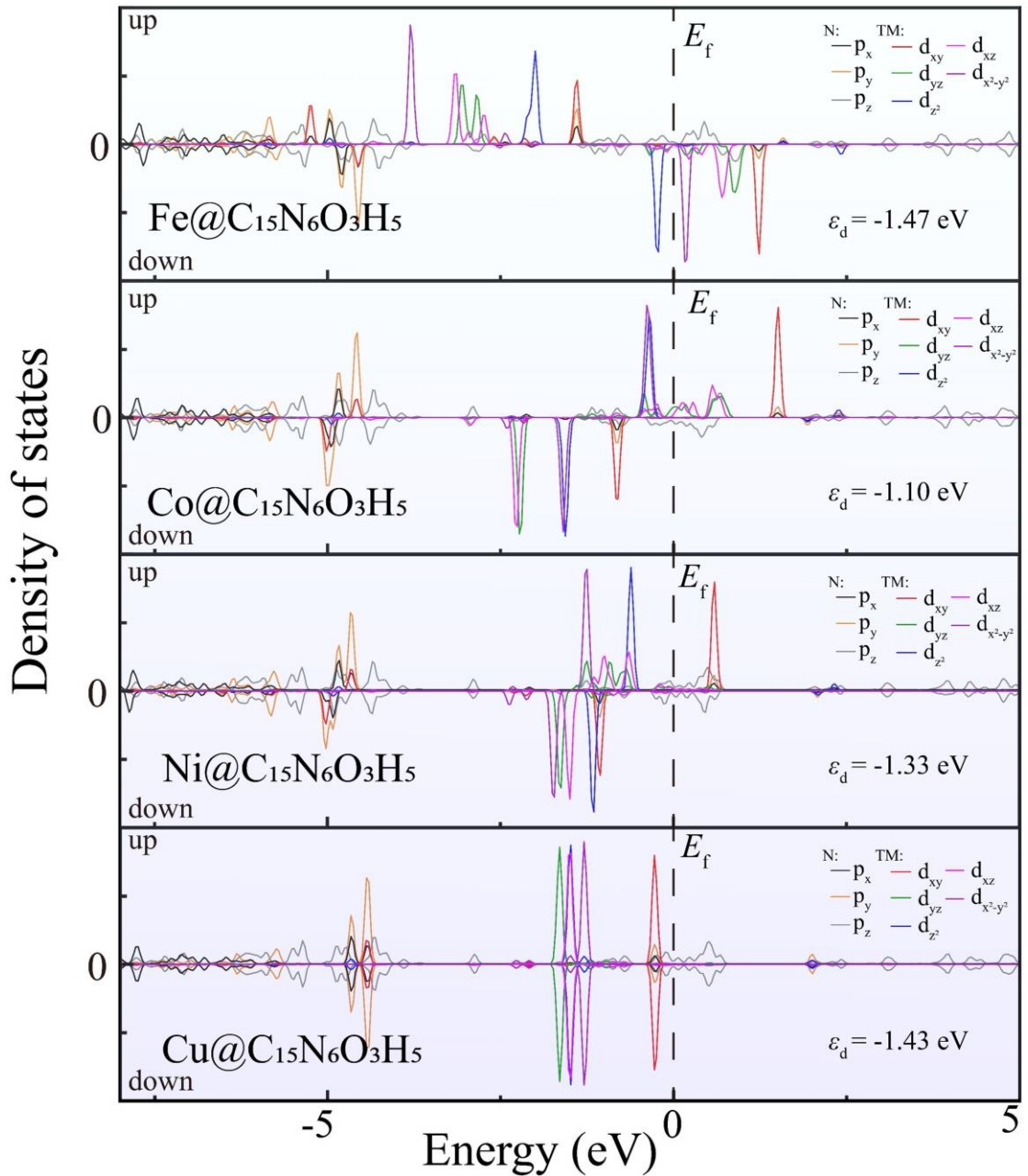


Fig. S16. PDOS diagrams for the $\text{Fe}@\text{C}_{15}\text{N}_6\text{O}_3\text{H}_5$, $\text{Co}@\text{C}_{15}\text{N}_6\text{O}_3\text{H}_5$, $\text{Ni}@\text{C}_{15}\text{N}_6\text{O}_3\text{H}_5$ and $\text{Cu}@\text{C}_{15}\text{N}_6\text{O}_3\text{H}_5$ monolayers, include the d orbitals of TM and the p orbitals of N bonded to the TM.

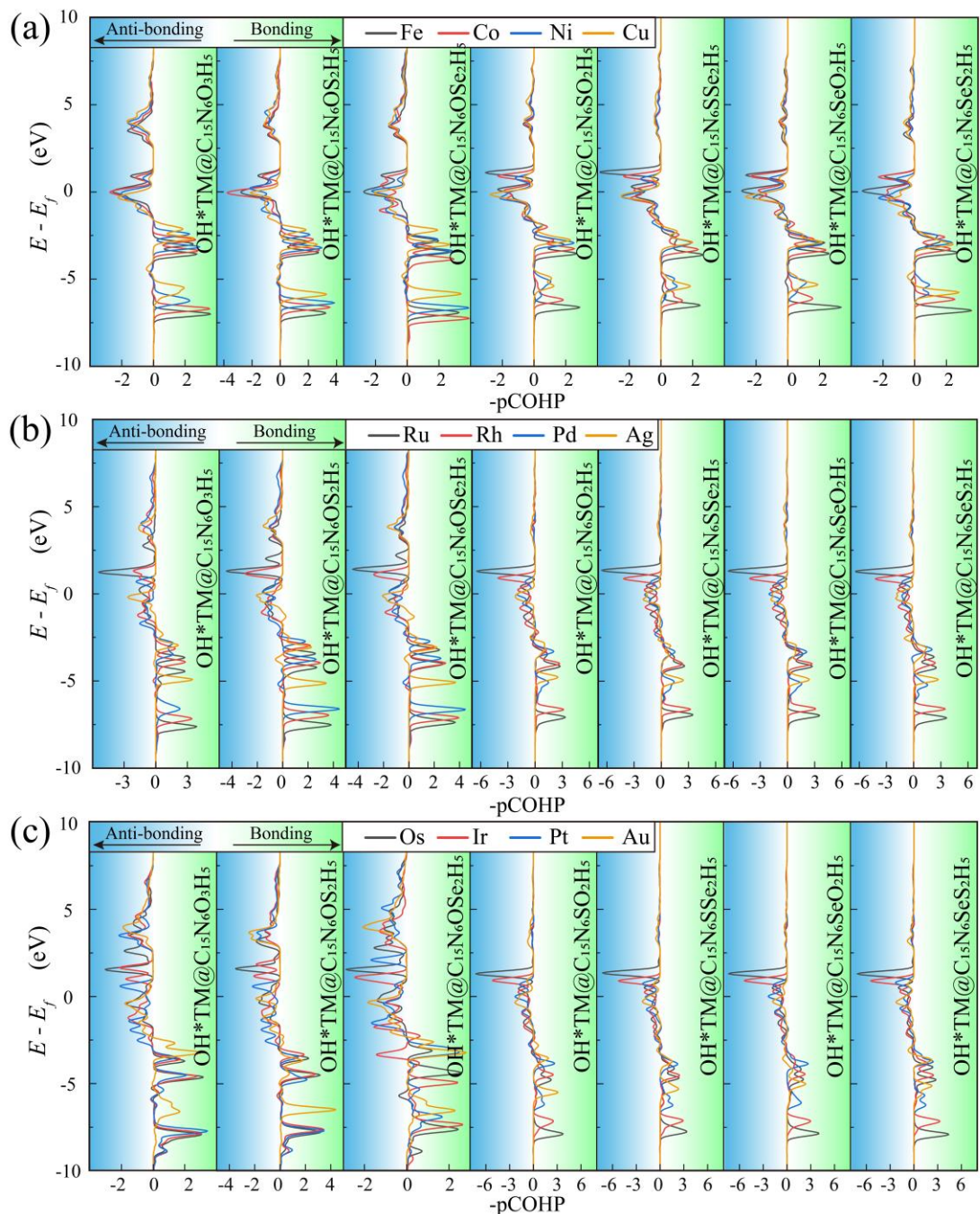


Fig. S17. pCOHP between the TM centers of (a) 3d, (b) 4d, and (c) 5d and the OH* intermediate for all seven configurations.

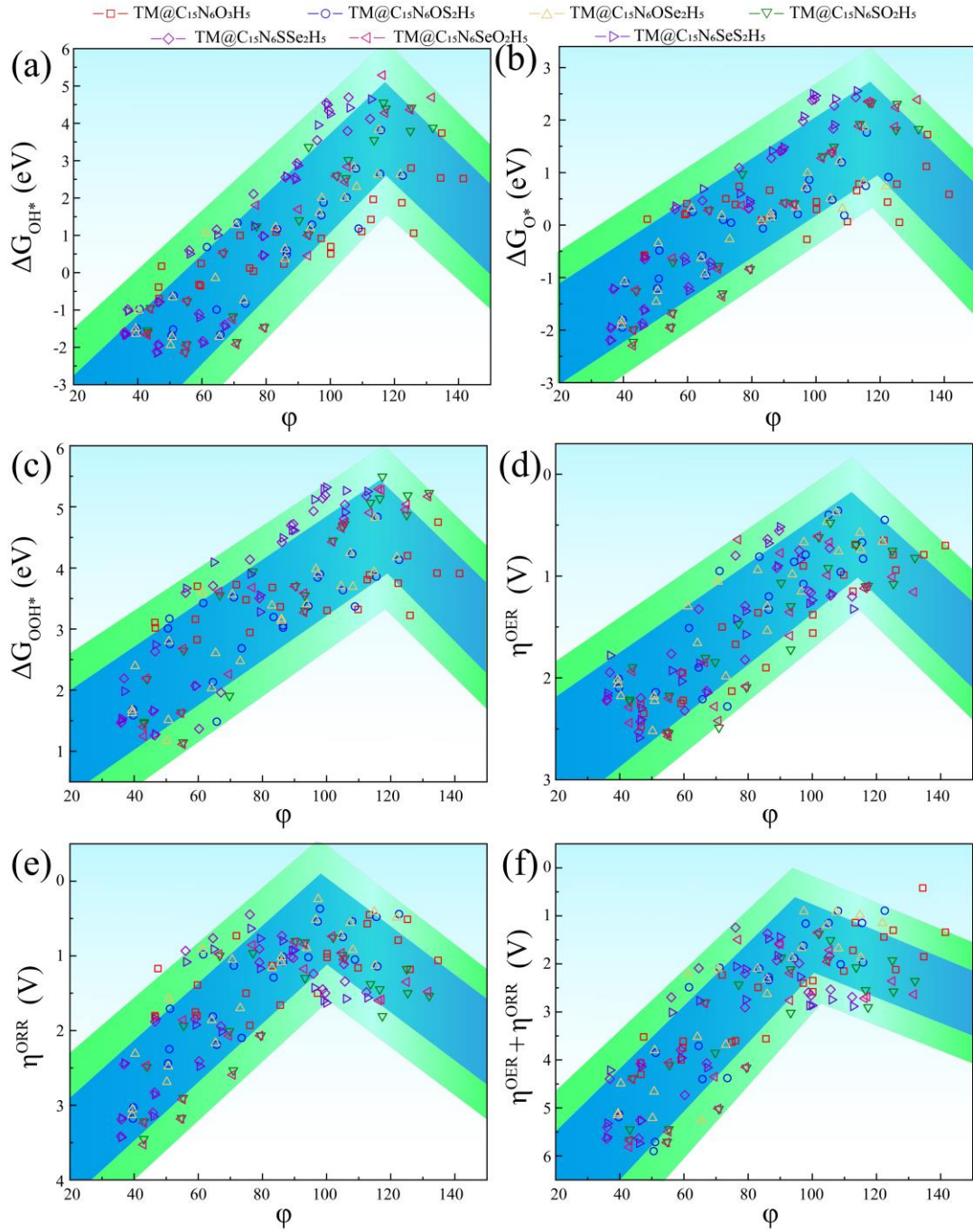


Fig. S18. The scaling relationship of (a) ΔG_{OH^*} , (b) ΔG_{O^*} , and (c) ΔG_{OOH^*} against the coordination descriptor φ . The Volcano maps of (d) the η^{OER} versus the coordination descriptor φ ; (e) the η^{ORR} against the coordination descriptor φ ; and (f) the overpotential of $(\eta^{\text{OER}} + \eta^{\text{ORR}})$ against the coordination descriptor.

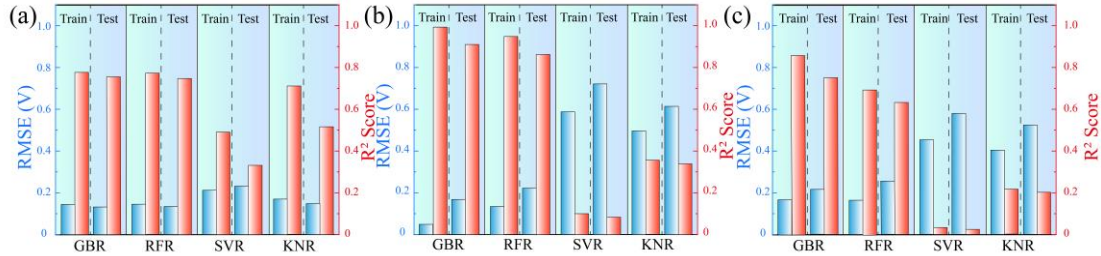


Fig. S19. The RMSE and R^2 results of the four ML algorithms in the training and test sets for (a) HER, (b) ORR and (c) OER.

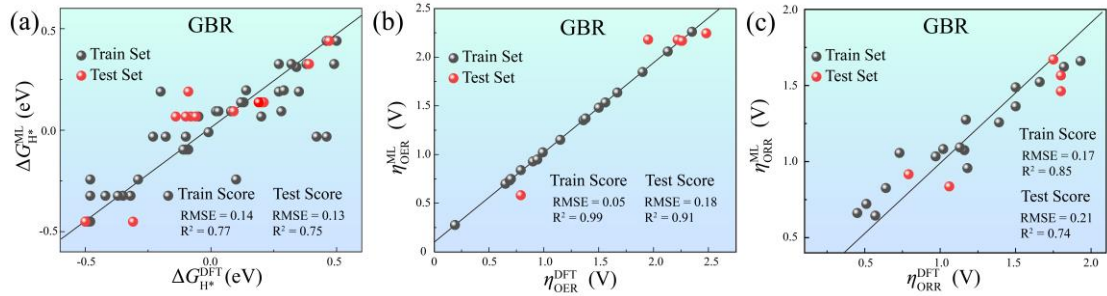


Fig. S20. A comparison of the DFT and GBR algorithms predicted overpotentials for (a)HER, (b) OER and (c) ORR.

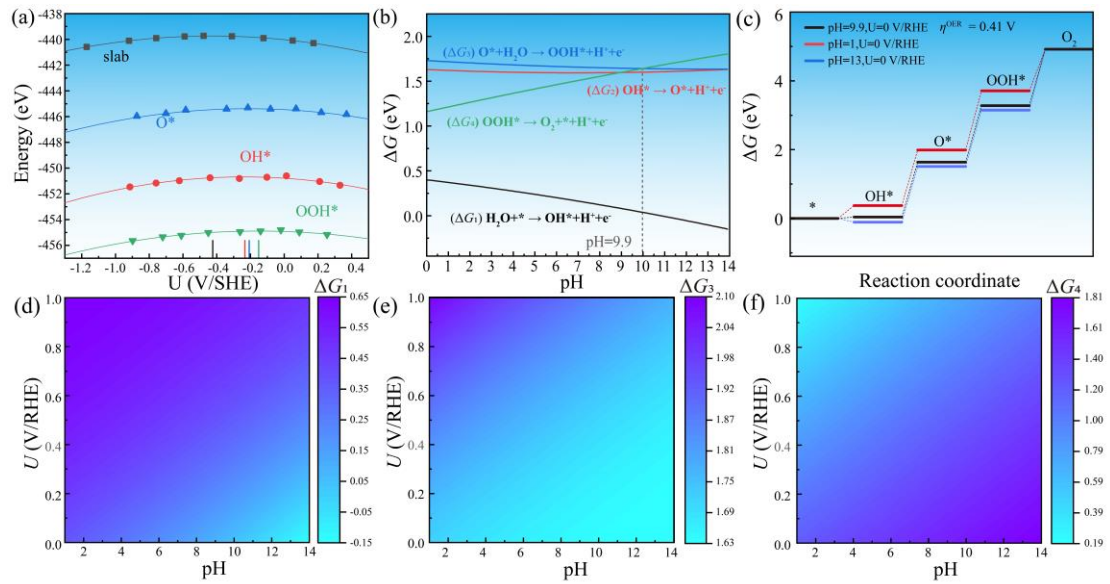


Fig. S21. (a) Calculated energies of the bare $\text{Au}@\text{C}_{15}\text{N}_6\text{OS}_2\text{H}_5$ slab and its three reaction intermediates ($^*\text{OOH}$, $^*\text{O}$, $^*\text{OH}$) as a function of the applied electrode potential. (b) Adsorption free energy changes of different ΔG relative to the applied pH value. (c) Free energy profiles catalyzed by $\text{Au}@\text{C}_{15}\text{N}_6\text{OS}_2\text{H}_5$ at different conditions: pH = 1, pH = 9.9 and pH = 13 (U = 0 V/RHE). Contour plots showing the dependency of (d) ΔG_1 , (e) ΔG_3 and (f) ΔG_4 on pH and applied potential for $\text{Au}@\text{C}_{15}\text{N}_6\text{OS}_2\text{H}_5$.

Table S1. The lattice geometric parameters of seven different monolayer configurations:lattice constants (a and b , Å) and interaxial angles (γ , deg).

Configurations Parameters \	$C_{15}N_6O_3H_5$	$C_{15}N_6OS_2H_5$	$C_{15}N_6OSe_2H_5$	$C_{15}N_6SO_2H_5$	$C_{15}N_6SSe_2H_5$	$C_{15}N_6SeO_2H_5$	$C_{15}N_6SeS_2H_5$
a	16.78	16.75	16.79	16.78	16.76	16.76	16.42
b	16.79	16.73	16.79	16.81	16.77	16.79	16.89
γ	119.91	119.98	119.95	119.89	119.93	119.90	119.07

Table S2. The lattice geometric parameters of different configurations: lattice constants(a and b , Å) and interaxial angles (γ , deg).

Configurations	TM@ $C_{15}N_6O_3H_5$			TM@ $C_{15}N_6OS_2H_5$			TM@ $C_{15}N_6OSe_2H_5$			TM@ $C_{15}N_6SO_2H_5$		
Parameters \ Supported TM	a	b	γ	a	b	γ	a	b	γ	a	b	γ
Ti	15.91	17.05	117.81	15.91	17.00	117.88	15.94	17.01	117.93	16.24	17.02	118.47
V	15.82	17.11	117.54	15.82	17.04	117.69	15.89	17.01	117.83	16.20	17.02	118.39
Cr	15.98	17.04	117.96	16.07	16.97	118.23	15.96	17.01	117.99	16.19	17.02	118.36
Mn	16.27	16.95	118.67	16.23	16.91	118.66	16.24	16.91	118.68	16.15	17.02	118.30
Fe	16.53	16.86	119.31	16.21	16.92	118.61	16.18	16.94	118.51	16.11	16.99	118.29
Co	16.76	16.80	119.86	16.22	16.93	118.62	16.66	16.78	119.70	16.12	16.98	118.31
Ni	16.78	16.79	119.91	16.64	16.76	119.70	16.63	16.78	119.65	16.11	16.99	118.27
Cu	16.78	16.79	119.91	16.73	16.74	119.92	16.67	16.79	119.71	16.14	17.02	118.28
Zr	16.02	17.07	117.97	16.04	16.99	118.16	16.00	17.04	117.99	16.38	17.00	118.78
Nb	16.00	17.02	118.02	15.99	17.01	118.02	15.93	17.02	117.88	16.30	17.02	118.59
Mo	15.99	17.04	117.97	16.01	16.99	118.11	16.15	16.96	118.41	16.26	17.03	118.50
Ru	16.37	16.91	118.91	16.47	16.82	119.27	16.39	16.86	119.04	16.19	17.02	118.38
Rh	16.43	16.88	119.08	16.39	16.85	119.07	16.30	16.89	118.83	16.18	17.02	118.36
Pd	16.78	16.79	119.91	16.66	16.75	119.78	16.65	16.80	119.65	16.17	17.03	118.32
Ag	16.78	16.79	119.91	16.71	16.77	119.83	16.66	16.81	119.65	16.51	16.87	119.27
Hf	15.94	17.05	117.85	16.02	17.01	118.08	15.98	17.03	117.96	16.35	17.00	118.72
Ta	15.90	17.10	117.70	15.80	17.12	117.46	15.92	17.02	117.86	16.28	17.02	118.55
W	15.88	17.05	117.77	15.91	17.02	117.85	15.92	17.02	117.86	16.26	17.01	118.52
Re	15.95	17.05	117.91	15.97	16.99	118.03	16.00	16.99	118.08	16.22	17.03	118.44
Os	16.16	16.99	118.36	16.20	16.94	118.52	16.18	16.93	118.51	16.19	17.02	118.38
Ir	16.15	16.98	118.36	16.11	16.95	118.38	16.12	16.95	118.37	16.18	17.01	118.36
Pt	16.78	16.79	119.91	16.65	16.77	119.70	16.05	16.99	118.17	16.16	17.02	118.31
Au	16.78	16.79	119.91	16.73	16.77	119.87	16.64	16.80	119.64	16.42	16.93	118.98

Configurations	TM@C ₁₅ N ₆ SSe ₂ H ₅			TM@C ₁₅ N ₆ SeO ₂ H ₅			TM@C ₁₅ N ₆ SeS ₂ H ₅		
Parameters Supported TM \	<i>a</i>	<i>b</i>	γ	<i>a</i>	<i>b</i>	γ	<i>a</i>	<i>b</i>	γ
Ti	16.36	16.89	118.94	16.51	16.87	119.25	16.57	16.77	119.56
V	16.35	16.88	118.94	16.49	16.85	119.24	16.53	16.80	119.43
Cr	16.34	16.87	118.93	16.49	16.84	119.27	16.49	16.81	119.34
Mn	16.36	16.87	118.98	16.53	16.85	119.32	16.56	16.77	119.54
Fe	16.20	16.92	118.58	16.52	16.83	119.34	16.50	16.79	119.39
Co	16.14	16.93	118.44	16.30	16.89	118.80	16.28	16.91	118.76
Ni	16.12	16.94	118.38	16.29	16.92	118.74	16.30	16.85	118.87
Cu	16.16	16.97	118.41	16.32	16.96	118.73	16.44	16.81	119.23
Zr	16.44	16.92	119.04	16.52	16.94	119.15	16.65	16.79	119.67
Nb	16.40	16.90	119.01	16.47	16.96	119.02	16.61	16.78	119.62
Mo	16.39	16.89	118.99	16.43	16.96	118.92	16.60	16.77	119.63
Ru	16.33	16.86	118.93	16.47	16.87	119.18	16.47	16.82	119.28
Rh	16.19	16.96	118.48	16.37	16.94	118.85	16.40	16.88	119.02
Pd	16.18	16.98	118.44	16.34	16.96	118.76	16.46	16.82	119.24
Ag	16.31	16.97	118.71	16.49	16.93	119.12	16.60	16.81	119.55
Hf	16.42	16.92	119.00	16.45	16.97	118.96	16.61	16.80	119.59
Ta	16.39	16.89	118.99	16.45	16.95	119.00	16.60	16.79	119.60
W	16.38	16.89	118.97	16.42	16.97	118.92	16.58	16.78	119.56
Re	16.34	16.88	118.92	16.40	16.96	118.89	16.55	16.79	119.47
Os	16.31	16.89	118.84	16.37	16.96	118.83	16.49	16.81	119.32
Ir	16.19	16.96	118.49	16.34	16.95	118.79	16.44	16.84	119.18
Pt	16.18	16.97	118.44	16.34	16.96	118.76	16.42	16.85	119.13
Au	16.29	16.97	118.68	16.37	16.97	118.79	16.53	16.81	119.41

Table S3. Machine learning eigenvalues: atomic number (Z), atomic mass (M_{TM}), atomic radius (r_{TM} , pm), d-electron count (θ), electronegativity (χ), electron affinity (E_{A} , eV), first ionization energy (E_{I} , eV), and environment feature (χ_{E}).

Eigenvalue Supported TM \	Z	M_{TM}	r_{TM}	θ	χ	E_{A}	E_{I}
Ti	22	47.87	147	4	1.54	0.08	6.83
V	23	50.94	134	5	1.63	0.53	6.75
Cr	24	52.00	128	6	1.66	0.68	6.77
Mn	25	54.94	127	7	1.55	0.97	7.43
Fe	26	55.85	124	8	1.83	0.15	7.90
Co	27	58.93	125	9	1.88	0.66	7.88
Ni	28	58.69	124	10	1.91	1.16	7.64
Cu	29	63.55	128	11	1.90	0.81	7.73
Zr	40	91.22	160	4	1.33	0.04	6.83
Nb	41	92.91	146	5	1.60	0.92	6.76
Mo	42	95.95	139	6	2.16	0.75	7.09
Ru	44	101.07	134	8	2.20	1.05	7.36
Rh	45	102.91	134	9	2.28	1.14	7.46
Pd	46	106.42	137	10	2.20	0.56	8.34
Ag	47	107.87	144	11	1.93	1.30	7.58
Hf	48	178.49	159	4	1.30	0.73	6.83
Ta	73	180.95	146	5	1.50	0.32	7.55
W	74	183.84	139	6	2.36	0.82	7.86
Re	75	186.21	137	7	1.90	0.60	7.83
Os	76	190.23	135	8	2.20	1.08	8.44
Ir	77	192.22	136	9	2.20	1.56	8.97
Pt	78	195.08	139	10	2.28	2.13	8.96
Au	79	196.97	144	11	2.54	2.31	9.23

Configurations Parameters \	TM@C ₁₅ N ₆ O ₃ H ₅	TM@C ₁₅ N ₆ OS ₂ H ₅	TM@C ₁₅ N ₆ OSe ₂ H ₅	TM@C ₁₅ N ₆ SO ₂ H ₅	TM@C ₁₅ N ₆ SSe ₂ H ₅	TM@C ₁₅ N ₆ SeO ₂ H ₅	TM@C ₁₅ N ₆ SeS ₂ H ₅
χ_{E}	10.32	8.6	8.54	9.46	7.68	9.43	7.71

Table S4. Calculated binding energies (E_b , in eV) of TM atoms anchored on different configurations.

Configurations Supported TM \	TM@C ₁₅ N ₆ O ₃ H ₅	TM@C ₁₅ N ₆ OS ₂ H ₅	TM@C ₁₅ N ₆ OSe ₂ H ₅	TM@C ₁₅ N ₆ SO ₂ H ₅	TM@C ₁₅ N ₆ SSe ₂ H ₅	TM@C ₁₅ N ₆ SeO ₂ H ₅	TM@C ₁₅ N ₆ SeS ₂ H ₅
Ti	-8.05	-8.10	-8.07	-8.59	-8.65	-8.54	-8.55
V	-6.72	-6.78	-6.73	-7.78	-7.77	-7.82	-7.84
Cr	-4.92	-4.92	-5.00	-6.37	-6.37	-6.39	-6.46
Mn	-4.37	-4.49	-4.50	-6.10	-5.83	-5.85	-5.89
Fe	-4.13	-4.47	-4.61	-6.21	-6.53	-6.11	-6.19
Co	-4.24	-4.45	-4.31	-6.89	-6.88	-7.08	-7.17
Ni	-4.30	-4.37	-4.40	-6.55	-6.58	-6.81	-6.87
Cu	-3.13	-3.13	-3.19	-4.51	-4.55	-4.78	-4.76
Zr	-9.31	-9.37	-9.37	-9.50	-9.56	-9.34	-9.42
Nb	-8.25	-8.36	-8.39	-8.65	-8.72	-8.57	-8.61
Mo	-5.63	-5.69	-5.60	-7.13	-7.20	-7.14	-7.17
Ru	-5.88	-5.84	-5.96	-8.36	-8.25	-8.50	-8.54
Rh	-4.97	-5.07	-5.18	-7.39	-7.45	-7.62	-7.69
Pd	-2.94	-2.98	-3.03	-5.23	-5.28	-5.55	-5.55
Ag	-2.41	-2.46	-2.52	-3.48	-3.46	-3.54	-3.66
Hf	-9.37	-9.40	-9.42	-9.54	-9.59	-9.34	-9.46
Ta	-9.31	-9.35	-9.35	-9.62	-9.69	-9.51	-9.52
W	-7.93	-7.81	-7.84	-9.15	-9.19	-9.10	-9.13
Re	-6.99	-7.00	-6.99	-8.96	-8.94	-9.06	-9.03
Os	-5.77	-5.82	-5.85	-8.67	-8.58	-8.83	-8.78
Ir	-5.72	-5.84	-5.87	-8.54	-8.60	-8.73	-8.76
Pt	-3.83	-3.89	-4.71	-7.40	-7.45	-7.66	-7.70
Au	-1.78	-1.81	-1.87	-3.30	-3.39	-3.68	-3.71

Table S5. Calculated charge exchange (Q , in e^-) of the TM atoms based on Bader charge analysis, where the negative values denote the charge transfer from the TM atom to the substrate. The electronegativity (χ) of different transition metals is indicated in parentheses.

Configurations TM(χ) \	TM@C ₁₅ N ₆ O ₃ H ₅	TM@C ₁₅ N ₆ OS ₂ H ₅	TM@C ₁₅ N ₆ OSe ₂ H ₅	TM@C ₁₅ N ₆ SO ₂ H ₅	TM@C ₁₅ N ₆ SSe ₂ H ₅	TM@C ₁₅ N ₆ SeO ₂ H ₅	TM@C ₁₅ N ₆ SeS ₂ H ₅
Ti (1.54)	-1.48	-1.49	-1.49	-1.42	-1.42	-1.37	-1.37
V (1.63)	-1.44	-1.45	-1.44	-1.24	-1.24	-1.19	-1.19
Cr (1.66)	-1.28	-1.28	-1.29	-1.18	-1.17	-1.12	-1.12
Mn (1.55)	-1.28	-1.30	-1.30	-1.19	-1.19	-1.11	-1.11
Fe (1.83)	-1.06	-1.13	-1.18	-0.80	-0.96	-1.00	-1.01
Co (1.88)	-0.83	-0.86	-0.78	-0.74	-0.74	-0.66	-0.66
Ni (1.92)	-0.89	-1.08	-0.76	-0.70	-0.71	-0.61	-0.60
Cu (1.90)	-0.68	-0.68	-0.70	-0.76	-0.76	-0.88	-0.67
Zr (1.33)	-1.81	-1.83	-1.84	-1.77	-1.77	-1.72	-1.69
Nb (1.59)	-1.76	-1.77	-1.77	-1.54	-1.55	-1.43	-1.40
Mo (2.16)	-1.36	-1.34	-1.28	-1.17	-1.17	-1.10	-1.10
Ru (2.20)	-0.72	-0.73	-0.75	-0.65	-0.66	-0.55	-0.56
Rh (2.28)	-0.63	-0.66	-0.67	-0.52	-0.54	-0.42	-0.43
Pd (2.20)	-0.54	-0.56	-0.56	-0.52	-0.54	-0.41	-0.42
Ag (1.93)	-0.63	-0.64	-0.64	-0.45	-0.43	-0.35	-0.36
Hf (1.32)	-1.66	-1.67	-1.67	-1.58	-1.60	-1.56	-1.54
Ta (1.51)	-1.75	-1.76	-1.73	-1.53	-1.55	-1.43	-1.41
W (2.36)	-1.63	-1.58	-1.60	-1.30	-1.29	-1.23	-1.21
Re (1.93)	-1.16	-1.21	-1.27	-1.02	-1.05	-0.93	-0.89
Os (2.18)	-0.83	-0.84	-0.84	-0.73	-0.73	-0.59	-0.61
Ir (2.20)	-0.71	-0.73	-0.73	-0.57	-0.59	-0.42	-0.45
Pt (2.28)	-0.47	-0.51	-0.77	-0.50	-0.50	-0.36	-0.37
Au (2.54)	-0.45	-0.47	-0.47	-0.45	-0.49	-0.46	-0.36

Table S6. The ML predictions of binding energies (E_b , in eV) of TM atoms anchored on different configurations.

Configurations Supported TM \	TM@C ₁₅ N ₆ O ₃ H ₅	TM@C ₁₅ N ₆ OS ₂ H ₅	TM@C ₁₅ N ₆ OSe ₂ H ₅	TM@C ₁₅ N ₆ SO ₂ H ₅	TM@C ₁₅ N ₆ SSe ₂ H ₅	TM@C ₁₅ N ₆ SeO ₂ H ₅	TM@C ₁₅ N ₆ SeS ₂ H ₅
Ti	-7.89	-7.13	-7.13	-8.52	-8.79	-8.55	-8.79
V	-6.71	-5.86	-5.86	-8.20	-8.62	-8.24	-8.62
Cr	-6.34	-6.13	-6.13	-6.34	-6.37	-6.34	-6.37
Mn	-6.13	-4.64	-4.66	-6.13	-4.90	-6.13	-4.90
Fe	-6.13	-4.74	-4.75	-6.13	-4.98	-6.13	-4.98
Co	-6.13	-4.72	-4.74	-6.13	-4.97	-6.13	-4.97
Ni	-3.39	-3.42	-3.42	-6.55	-6.89	-6.81	-6.83
Cu	-3.42	-3.45	-3.45	-3.42	-4.70	-3.42	-4.70
Zr	-8.96	-9.13	-9.12	-9.24	-9.11	-9.24	-9.11
Nb	-7.41	-6.84	-6.84	-8.54	-8.80	-8.57	-8.80
Mo	-6.88	-6.54	-6.54	-8.44	-8.76	-8.47	-8.76
Ru	-6.50	-5.86	-5.86	-8.20	-8.36	-8.24	-8.36
Rh	-6.30	-5.87	-5.87	-8.24	-8.40	-8.28	-8.40
Pd	-3.22	-3.25	-3.25	-3.22	-6.29	-3.22	-6.24
Ag	-3.44	-3.38	-3.46	-3.44	-6.17	-3.44	-6.14
Hf	-8.80	-8.95	-8.95	-9.19	-9.09	-9.19	-9.09
Ta	-8.86	-9.11	-9.11	-9.24	-9.10	-9.24	-9.10
W	-6.79	-6.52	-6.52	-8.49	-8.76	-8.52	-8.76
Re	-6.92	-6.50	-6.50	-8.46	-8.81	-8.50	-8.81
Os	-6.05	-5.86	-5.86	-8.34	-8.47	-8.39	-8.47
Ir	-5.80	-5.88	-5.88	-8.49	-8.57	-8.54	-8.57
Pt	-4.09	-4.09	-4.85	-7.40	-7.36	-7.66	-7.30
Au	-3.90	-2.24	-2.24	-3.90	-3.39	-3.90	-6.41

Table S7. The ML predictions of charge exchange (Q , in e^-) of the TM atoms based on Bader charge analysis, where the negative values denote the charge transfer from the TM atom to the substrate.

Configurations TM(χ) \	TM@C ₁₅ N ₆ O ₃ H ₅	TM@C ₁₅ N ₆ OS ₂ H ₅	TM@C ₁₅ N ₆ OSe ₂ H ₅	TM@C ₁₅ N ₆ SO ₂ H ₅	TM@C ₁₅ N ₆ SSe ₂ H ₅	TM@C ₁₅ N ₆ SeO ₂ H ₅	TM@C ₁₅ N ₆ SeS ₂ H ₅
Ti (1.54)	-1.50	-1.44	-1.44	-1.45	-1.44	-1.45	-1.44
V (1.63)	-1.41	-1.35	-1.36	-1.35	-1.35	-1.35	-1.35
Cr (1.66)	-1.30	-1.26	-1.26	-1.24	-1.25	-1.25	-1.25
Mn (1.55)	-1.33	-1.29	-1.30	-1.27	-1.28	-1.28	-1.28
Fe (1.83)	-0.90	-1.07	-1.10	-0.88	-0.96	-0.96	-0.95
Co (1.88)	-0.86	-1.01	-1.02	-0.84	-0.85	-0.90	-0.84
Ni (1.92)	-0.80	-0.97	-0.96	-0.78	-0.75	-0.84	-0.73
Cu (1.90)	-0.87	-1.01	-1.02	-0.85	-0.82	-0.91	-0.81
Zr (1.33)	-1.75	-1.71	-1.71	-1.72	-1.71	-1.72	-1.71
Nb (1.59)	-1.63	-1.58	-1.58	-1.58	-1.57	-1.58	-1.57
Mo (2.16)	-1.23	-1.21	-1.21	-1.18	-1.18	-1.18	-1.18
Ru (2.20)	-0.66	-0.80	-0.79	-0.64	-0.70	-0.65	-0.70
Rh (2.28)	-0.60	-0.76	-0.75	-0.58	-0.65	-0.59	-0.64
Pd (2.20)	-0.60	-0.74	-0.73	-0.58	-0.65	-0.59	-0.64
Ag (1.93)	-0.55	-0.74	-0.73	-0.53	-0.62	-0.54	-0.61
Hf (1.32)	-1.72	-1.68	-1.68	-1.69	-1.68	-1.68	-1.68
Ta (1.51)	-1.69	-1.64	-1.64	-1.64	-1.64	-1.64	-1.64
W (2.36)	-1.22	-1.21	-1.21	-1.17	-1.18	-1.17	-1.18
Re (1.93)	-1.26	-1.22	-1.24	-1.19	-1.22	-1.20	-1.22
Os (2.18)	-0.57	-0.73	-0.73	-0.56	-0.65	-0.56	-0.65
Ir (2.20)	-0.45	-0.64	-0.64	-0.44	-0.52	-0.44	-0.52
Pt (2.28)	-0.54	-0.73	-0.72	-0.54	-0.62	-0.54	-0.61
Au (2.54)	-0.51	-0.70	-0.70	-0.50	-0.60	-0.50	-0.60

Table S8. Calculated Gibbs free energies (ΔG_{H^*} , in eV) of H^* on different configurations and the results of screening based on the absolute value of ΔG_{H^*} less than 0.09 eV are highlighted in blue.

Configurations Supported TM \ \diagdown	TM@C ₁₅ N ₆ O ₃ H ₅	TM@C ₁₅ N ₆ OS ₂ H ₅	TM@C ₁₅ N ₆ OSe ₂ H ₅	TM@C ₁₅ N ₆ SO ₂ H ₅	TM@C ₁₅ N ₆ SSe ₂ H ₅	TM@C ₁₅ N ₆ SeO ₂ H ₅	TM@C ₁₅ N ₆ SeS ₂ H ₅
Ti	1.19	-0.10	-0.11	-0.11	-0.09	-0.11	-0.10
V	1.26	0.12	0.13	0.19	0.21	0.20	0.21
Cr	1.28	0.52	0.53	0.76	0.50	0.46	0.47
Mn	0.67	0.68	0.67	0.52	0.34	2.54	0.62
Fe	0.75	0.46	0.63	-0.10	0.42	-0.23	-0.18
Co	0.39	0.56	0.49	0.38	0.32	0.32	0.27
Ni	0.57	0.72	0.74	1.17	1.19	1.07	1.06
Cu	0.67	0.76	0.80	1.16	1.12	1.09	0.98
Zr	3.84	-0.48	-0.51	-0.51	-0.51	-0.54	-0.50
Nb	0.93	-0.31	-0.50	-0.53	-0.53	-0.52	-0.49
Mo	0.65	-0.55	-0.68	-0.35	-0.32	-0.37	-0.35
Ru	-0.17	-0.53	-0.66	-0.42	-0.55	-0.48	-0.53
Rh	0.58	0.28	0.68	0.09	0.08	0.03	0.02
Pd	0.97	1.06	1.06	1.32	1.32	1.22	1.19
Ag	1.14	1.31	1.33	1.48	1.32	1.20	1.18
Hf	0.67	-0.66	-0.67	-0.73	-0.72	-0.80	-0.72
Ta	0.90	-0.49	-0.74	-0.81	-0.79	-0.79	-0.79
W	1.13	-0.78	-0.83	-0.73	-0.72	-0.76	-0.74
Re	0.70	-0.01	-0.70	-0.79	-0.79	-0.88	-0.88
Os	0.1	-0.29	-0.59	-0.48	-0.61	-0.52	-0.6
Ir	0.57	0.20	-0.06	-0.05	-0.08	-0.1	-0.14
Pt	0.14	0.29	0.89	0.91	0.91	0.82	0.79
Au	-0.2	-0.09	1.2	0.24	0.27	0.58	0.35

Table S9. Calculated the Gibbs free energies (ΔG_{OH^*} , in eV) of OH* on different configurations, where the results with negative ΔG_{OH^*} are highlighted in red.

Configurations Supported TM \	TM@C ₁₅ N ₆ O ₃ H ₅	TM@C ₁₅ N ₆ OS ₂ H ₅	TM@C ₁₅ N ₆ OSe ₂ H ₅	TM@C ₁₅ N ₆ SO ₂ H ₅	TM@C ₁₅ N ₆ SSe ₂ H ₅	TM@C ₁₅ N ₆ SeO ₂ H ₅	TM@C ₁₅ N ₆ SeS ₂ H ₅
Ti	0.11	-1.10	-1.08	-1.26	-1.22	-1.24	-1.21
V	0.41	-0.48	-0.34	-0.70	-0.65	-0.63	-0.61
Cr	0.50	0.25	0.32	0.29	0.30	0.28	0.36
Mn	0.10	0.10	0.18	0.97	0.47	0.38	0.69
Fe	-0.27	-0.06	0.07	0.43	1.09	0.41	0.60
Co	0.07	0.21	0.34	1.31	1.27	1.28	1.41
Ni	0.44	0.48	0.50	1.92	1.98	1.88	2.07
Cu	1.12	0.75	0.82	1.81	1.83	1.87	1.91
Zr	-0.59	-1.80	-1.83	-1.99	-1.96	-2.00	-1.94
Nb	0.22	-1.02	-1.25	-1.67	-1.60	-1.69	-1.63
Mo	0.39	-0.58	-0.63	-0.78	-0.62	-0.84	-0.69
Ru	0.44	0.15	0.21	0.41	0.32	0.39	0.46
Rh	0.78	0.86	0.99	1.49	1.43	1.42	1.48
Pd	0.78	1.19	1.21	2.33	2.38	2.35	2.50
Ag	1.72	1.76	1.85	2.31	2.27	2.24	2.40
Hf	-0.57	-1.95	-1.90	-2.22	-2.19	-2.30	-2.20
Ta	0.20	-1.21	-1.46	-1.94	-1.87	-1.95	-1.92
W	0.74	-0.96	-0.94	-1.30	-1.18	-1.36	-1.25
Re	0.66	0.04	-0.27	-0.84	-0.71	-0.84	-0.78
Os	0.30	0.22	0.14	0.41	0.31	0.40	0.41
Ir	0.66	0.69	0.71	1.38	1.41	1.38	1.41
Pt	0.05	0.18	0.31	2.33	2.39	2.33	2.47
Au	0.59	0.91	0.74	1.83	2.43	2.39	2.55

Table S10. Calculated the Gibbs free energies (ΔG_{O^*} , in eV) of O^* on different configurations, where the red refers to structures that have been excluded.

Configurations Supported TM \	TM@C ₁₅ N ₆ O ₃ H ₅	TM@C ₁₅ N ₆ OS ₂ H ₅	TM@C ₁₅ N ₆ OSe ₂ H ₅	TM@C ₁₅ N ₆ SO ₂ H ₅	TM@C ₁₅ N ₆ SSe ₂ H ₅	TM@C ₁₅ N ₆ SeO ₂ H ₅	TM@C ₁₅ N ₆ SeS ₂ H ₅
Ti	0.17	-0.98	-1.01	-0.95	-0.98	-0.97	-1.03
V	0.25	-0.62	-0.66	-0.76	-0.79	-0.75	-0.79
Cr	1.00	0.69	1.07	0.52	0.60	0.53	0.51
Mn	1.09	1.34	1.28	1.24	1.15	1.81	1.01
Fe	0.92	1.16	1.21	1.41	2.11	1.69	1.25
Co	1.10	1.29	1.19	2.60	2.55	2.59	2.58
Ni	1.87	2.01	2.00	3.55	3.55	6.87	3.95
Cu	2.54	2.65	2.63	3.79	3.79	-1.66	9.51
Zr	-0.69	-1.61	-1.64	-1.60	-1.66	-1.67	-1.67
Nb	-0.35	-1.52	-1.72	-1.92	-1.92	-1.94	-1.95
Mo	0.12	-0.99	-0.14	-1.17	-1.10	-1.25	-1.20
Ru	0.70	0.59	0.63	1.03	0.98	1.00	0.98
Rh	1.96	1.88	2.00	3.02	2.93	2.84	2.87
Pd	2.80	2.79	2.82	4.55	4.54	5.29	4.49
Ag	3.74	3.82	3.83	4.42	4.69	4.36	4.41
Hf	-0.39	-1.49	-1.50	-1.55	-1.59	-1.65	-1.63
Ta	-0.32	-1.68	-1.94	-2.13	-2.11	-2.14	-2.15
W	0.04	-1.67	-1.72	-1.86	-1.83	-1.92	-1.89
Re	0.23	-0.83	-0.74	-1.45	-1.40	-1.48	-1.45
Os	0.51	0.49	0.37	3.37	0.45	0.45	0.47
Ir	1.42	1.53	1.60	2.53	2.55	2.43	2.49
Pt	1.06	1.18	2.30	4.39	4.33	4.28	4.25
Au	2.52	2.59	2.63	3.88	4.12	4.69	4.65

Table S11. Calculated the Gibbs free energies (ΔG_{OOH^*} , in eV) of OOH* on different configurations, where the red refers to structures that have been excluded.

Configurations Supported TM \	TM@C ₁₅ N ₆ O ₃ H ₅	TM@C ₁₅ N ₆ OS ₂ H ₅	TM@C ₁₅ N ₆ OSe ₂ H ₅	TM@C ₁₅ N ₆ SO ₂ H ₅	TM@C ₁₅ N ₆ SSe ₂ H ₅	TM@C ₁₅ N ₆ SeO ₂ H ₅	TM@C ₁₅ N ₆ SeS ₂ H ₅
Ti	3.75	9.04	2.40	2.18	2.19	2.19	1.98
V	3.70	2.75	2.80	2.64	2.63	2.68	2.74
Cr	3.73	3.43	3.60	3.56	3.59	3.61	3.66
Mn	3.68	3.52	3.56	3.94	3.71	3.68	4.09
Fe	3.04	3.20	3.38	3.70	4.14	3.70	3.90
Co	3.32	3.37	3.40	4.45	4.42	4.43	4.49
Ni	3.75	3.64	3.70	5.07	4.93	4.90	5.12
Cu	3.92	3.86	3.93	4.87	4.80	4.95	4.91
Zr	3.02	1.59	1.63	1.46	1.48	1.25	1.54
Nb	2.83	3.17	1.51	1.15	1.26	1.11	1.28
Mo	3.48	2.13	2.03	1.91	2.07	2.26	2.07
Ru	3.30	3.02	3.16	3.55	3.50	3.59	3.55
Rh	3.88	3.90	3.90	4.72	4.72	4.74	4.61
Pd	4.20	4.23	4.24	5.14	5.14	5.29	5.29
Ag	4.75	4.83	4.82	5.19	5.03	5.04	5.26
Hf	3.11	1.68	1.67	1.48	1.47	1.40	1.51
Ta	3.16	3.01	1.17	1.63	1.65	1.63	1.67
W	2.94	1.48	2.61	1.20	1.37	1.27	-2.24
Re	3.36	2.68	2.48	1.60	1.96	1.61	1.93
Os	3.30	3.06	3.13	3.30	3.51	3.27	3.28
Ir	3.81	3.84	3.98	4.68	4.7	4.65	4.62
Pt	3.22	3.37	3.69	5.5	5.19	5.27	5.32
Au	3.91	4.13	4.17	5.23	5.18	5.17	5.25

Table S12. The pre-screening factor (P_{sf}) of different configurations and the results with $P_{sf} > 0.55$ are highlighted in red and corresponding structures no longer were considered. Herein, the “/” represents that the configurations were filtered out in the former screening processes.

Configurations Supported TM \	TM@C ₁₅ N ₆ O ₃ H ₅	TM@C ₁₅ N ₆ OS ₂ H ₅	TM@C ₁₅ N ₆ OSe ₂ H ₅	TM@C ₁₅ N ₆ SO ₂ H ₅	TM@C ₁₅ N ₆ SSe ₂ H ₅	TM@C ₁₅ N ₆ SeO ₂ H ₅	TM@C ₁₅ N ₆ SeS ₂ H ₅
Ti	1.14	/	/	/	/	/	/
V	1.11	/	/	/	/	/	/
Cr	0.73	0.89	0.69	0.97	0.93	0.96	0.98
Mn	0.69	0.56	0.59	0.61	0.65	0.33	0.73
Fe	/	/	0.62	0.53	0.18	0.38	0.61
Co	0.68	0.59	0.64	0.07	0.05	0.06	0.06
Ni	0.29	0.23	0.23	0.54	0.54	2.20	0.75
Cu	0.04	0.09	0.08	0.67	0.67	7.56	6.53
Zr	/	/	/	/	/	/	/
Nb	1.41	/	/	/	/	/	/
Mo	1.17	/	/	/	/	/	/
Ru	0.88	0.93	0.91	0.72	0.74	0.73	0.74
Rh	0.25	0.29	0.23	0.28	0.24	0.19	0.20
Pd	0.17	0.16	0.18	1.05	1.04	1.41	1.02
Ag	0.64	0.68	0.68	0.98	1.12	0.95	0.98
Hf	/	/	/	/	/	/	/
Ta	1.39	/	/	/	/	/	/
W	1.21	/	/	/	/	/	/
Re	1.11	1.64	/	/	/	/	/
Os	0.98	0.98	1.05	0.45	1.00	1.00	0.99
Ir	0.52	0.46	0.43	0.03	0.04	0.02	0.01
Pt	0.70	0.64	0.08	0.97	0.94	0.91	0.90
Au	0.03	0.07	0.09	0.71	0.83	1.12	1.09

Table S13. Calculated OER overpotentials (η^{OER} , in V) of different configurations and the results with $\eta^{\text{OER}} < 0.55$ V are highlighted in blue. The configurations filtered out in the former screening are highlighted in red.

Configurations Supported TM \	TM@C ₁₅ N ₆ O ₃ H ₅	TM@C ₁₅ N ₆ OS ₂ H ₅	TM@C ₁₅ N ₆ OSe ₂ H ₅	TM@C ₁₅ N ₆ SO ₂ H ₅	TM@C ₁₅ N ₆ SSe ₂ H ₅	TM@C ₁₅ N ₆ SeO ₂ H ₅	TM@C ₁₅ N ₆ SeS ₂ H ₅
Ti	2.35	8.79	2.18	1.90	1.95	1.94	1.78
V	2.22	2.14	2.23	2.17	2.20	2.20	2.30
Cr	1.50	1.51	1.30	1.80	1.76	1.85	1.93
Mn	1.36	0.95	1.06	1.47	1.32	0.64	1.86
Fe	0.90	0.81	0.94	1.07	0.80	0.77	1.42
Co	0.99	0.86	0.98	0.62	0.64	0.61	0.68
Ni	0.65	0.40	0.47	0.69	0.75	3.75	0.84
Cu	0.19	0.67	0.58	0.75	0.73	16.38	12.37
Zr	2.48	2.10	2.06	2.23	2.21	2.44	2.15
Nb	1.95	3.46	2.18	2.54	2.43	2.58	2.41
Mo	2.13	1.90	1.66	1.84	1.95	2.28	2.03
Ru	1.38	1.20	1.30	1.30	1.29	1.35	1.34
Rh	0.69	0.79	0.67	0.48	0.56	0.67	0.52
Pd	0.79	0.36	0.37	1.10	1.15	1.12	1.27
Ag	0.79	0.83	0.74	1.08	1.19	1.01	1.17
Hf	2.26	2.01	2.02	2.21	2.22	2.29	2.18
Ta	2.25	3.46	2.52	2.53	2.53	2.54	2.59
W	1.67	2.21	3.09	2.49	2.32	2.42	5.93
Re	1.90	2.28	1.99	2.09	2.13	2.08	2.15
Os	1.56	1.33	1.54	1.72	1.82	1.59	1.58
Ir	1.15	1.08	1.15	0.92	0.92	0.99	0.90
Pt	0.94	0.96	0.76	1.10	1.16	1.10	1.24
Au	0.70	0.45	0.66	0.82	1.20	1.16	1.32

Table S14. Calculated ORR overpotentials (η^{ORR} , in V) of different configurations and the results with $\eta^{\text{ORR}} < 0.45$ V are highlighted in blue. The configurations filtered out in the former screening are highlighted in red.

Configurations Supported TM \	TM@C ₁₅ N ₆ O ₃ H ₅	TM@C ₁₅ N ₆ OS ₂ H ₅	TM@C ₁₅ N ₆ OSe ₂ H ₅	TM@C ₁₅ N ₆ SO ₂ H ₅	TM@C ₁₅ N ₆ SSe ₂ H ₅	TM@C ₁₅ N ₆ SeO ₂ H ₅	TM@C ₁₅ N ₆ SeS ₂ H ₅
Ti	1.17	5.35	2.31	2.49	2.45	2.47	2.44
V	1.39	1.71	1.57	1.93	1.88	1.86	1.84
Cr	0.73	0.98	0.91	1.00	0.93	0.98	1.08
Mn	1.13	1.13	1.05	0.96	0.76	0.85	0.91
Fe	1.50	1.29	1.16	0.80	0.45	0.82	0.63
Co	1.16	1.02	0.89	0.76	0.73	0.74	0.80
Ni	0.79	0.75	0.73	1.38	1.24	3.19	1.43
Cu	0.23	0.48	0.41	1.18	1.11	15.77	11.84
Zr	1.82	3.03	3.06	3.22	3.19	3.23	3.17
Nb	1.80	2.25	2.48	2.90	2.83	2.92	2.86
Mo	1.50	1.81	1.86	2.01	1.85	2.07	1.92
Ru	0.97	1.08	1.02	0.82	0.91	0.84	0.77
Rh	0.45	0.37	0.24	1.03	1.03	1.05	0.92
Pd	0.51	0.54	0.55	1.45	1.45	1.60	1.60
Ag	1.06	1.14	1.13	1.50	1.34	1.35	1.57
Hf	1.80	3.18	3.13	3.45	3.42	3.53	3.43
Ta	1.75	2.44	2.69	3.17	3.10	3.18	3.15
W	1.93	2.19	2.17	2.53	2.41	2.59	2.48
Re	1.66	2.10	1.70	2.07	1.94	2.07	2.01
Os	1.02	1.01	1.09	1.30	1.09	1.17	1.17
Ir	0.57	0.54	0.52	0.99	1.01	0.96	0.93
Pt	1.18	1.05	0.92	1.81	1.50	1.58	1.63
Au	0.64	0.44	0.49	1.54	1.49	1.48	1.56

Table S15. Δq , E_{VASP} , E_f , $E_{\text{FermiShift}}$, corresponding U and potential-dependent electrochemical energy E for Cu@C₁₅N₆O₃H₅. And the fitted $E-U$ relation is $E = -1.40U^2 - 2.25U - 452.60$, $R^2 = 0.99$.

Δq (e)	E_{VASP} (eV)	E_f (eV)	$E_{\text{FermiShift}}$ (eV)	U (V vs SHE)	E (eV)
-2.00	-442.96	-4.71	0.21	-0.11	-452.37
-1.50	-445.29	-4.55	0.21	-0.26	-452.11
-1.00	-447.54	-4.34	0.21	-0.47	-451.88
-0.50	-449.66	-4.14	0.21	-0.67	-451.73
0.00	-451.70	-3.96	0.21	-0.85	-451.70
0.50	-453.65	-3.79	0.21	-1.02	-451.76
1.00	-455.53	-3.62	0.21	-1.19	-451.90
1.50	-457.32	-3.45	0.21	-1.36	-452.14
2.00	-459.01	-3.27	0.21	-1.54	-452.47

Table S16. Δq , E_{VASP} , E_f , $E_{\text{FermiShift}}$, corresponding U and potential-dependent electrochemical energy E for OH*Cu@C₁₅N₆O₃H₅. And the fitted $E-U$ relation is $E = -1.34U^2 - 1.56U - 465.17$, $R^2 = 0.99$.

Δq (e)	E_{VASP} (eV)	E_f (eV)	$E_{\text{FermiShift}}$ (eV)	U (V vs SHE)	E (eV)
-2.00	-453.52	-4.90	0.21	0.08	-463.31
-1.50	-455.94	-4.73	0.21	-0.09	-463.04
-1.00	-458.29	-4.58	0.21	-0.24	-462.86
-0.50	-460.56	-4.41	0.21	-0.41	-462.76
0.00	-462.74	-4.19	0.21	-0.63	-462.74
0.50	-464.78	-3.99	0.21	-0.83	-462.79
1.00	-466.76	-3.82	0.21	-1.00	-462.94
1.50	-468.64	-3.65	0.21	-1.16	-463.16
2.00	-470.45	-3.48	0.21	-1.33	-463.48

Table S17. Δq , E_{VASP} , E_f , $E_{\text{FermiShift}}$, corresponding U and potential-dependent electrochemical energy E for $\text{O}^*\text{Cu}@\text{C}_{15}\text{N}_6\text{O}_3\text{H}_5$. And the fitted $E-U$ relation is $E = -1.35U^2 - 1.41U - 457.81$, $R^2 = 0.97$.

Δq (e)	E_{VASP} (eV)	E_f (eV)	$E_{\text{FermiShift}}$ (eV)	U (V vs SHE)	E (eV)
-2.00	-448.13	-4.95	0.21	0.14	-458.04
-1.50	-450.58	-4.79	0.21	-0.02	-457.77
-1.00	-452.95	-4.64	0.21	-0.18	-457.58
-0.50	-455.24	-4.49	0.21	-0.33	-457.48
0.00	-457.46	-4.28	0.21	-0.54	-457.46
0.50	-459.55	-4.06	0.21	-0.75	-457.51
1.00	-461.54	-3.89	0.21	-0.93	-457.65
1.50	-463.45	-3.72	0.21	-1.09	-457.87

Table S18. Δq , E_{VASP} , E_f , $E_{\text{FermiShift}}$, corresponding U and potential-dependent electrochemical energy E for $\text{OOH}^*\text{Cu}@\text{C}_{15}\text{N}_6\text{O}_3\text{H}_5$. And the fitted $E-U$ relation is $E = -1.45U^2 - 1.77U - 467.53$, $R^2 = 0.99$.

Δq (e)	E_{VASP} (eV)	E_f (eV)	$E_{\text{FermiShift}}$ (eV)	U (V vs SHE)	E (eV)
-2.00	-457.90	-4.83	0.22	0.02	-467.56
-1.50	-460.28	-4.70	0.22	-0.12	-467.33
-1.00	-462.60	-4.54	0.22	-0.28	-467.14
-0.50	-464.83	-4.39	0.22	-0.43	-467.03
0.00	-467.01	-4.19	0.22	-0.63	-467.01
0.50	-469.05	-3.98	0.22	-0.84	-467.06
1.00	-471.01	-3.82	0.22	-1.00	-467.20
1.50	-472.90	-3.66	0.22	-1.16	-467.41
2.00	-474.71	-3.50	0.22	-1.32	-467.72

Table S19. Δq , E_{VASP} , E_f , $E_{\text{FermiShift}}$, corresponding U and potential-dependent electrochemical energy E for Au@C₁₅N₆OS₂H₅. And the fitted $E-U$ relation is $E = -1.56U^2 - 1.34U - 440.02$, $R^2 = 0.99$.

Δq (e)	E_{VASP} (eV)	E_f (eV)	$E_{\text{FermiShift}}$ (eV)	U (V vs SHE)	E (eV)
-2.00	-430.29	-5.00	0.23	0.17	-440.29
-1.50	-432.78	-4.88	0.23	0.05	-440.09
-1.00	-435.20	-4.70	0.23	-0.12	-439.90
-0.50	-437.51	-4.49	0.23	-0.33	-439.75
0.00	-439.73	-4.35	0.23	-0.48	-439.73
0.50	-441.88	-4.21	0.23	-0.62	-439.78
1.00	-443.97	-4.07	0.23	-0.76	-439.90
1.50	-445.99	-3.90	0.23	-0.92	-440.13
2.00	-447.90	-3.66	0.23	-1.17	-440.59

Table S20. Δq , E_{VASP} , E_f , $E_{\text{FermiShift}}$, corresponding U and potential-dependent electrochemical energy E for OH*Au@C₁₅N₆OS₂H₅. And the fitted $E-U$ relation is $E = -1.56U^2 - 2.87U - 450.61$, $R^2 = 0.99$.

Δq (e)	E_{VASP} (eV)	E_f (eV)	$E_{\text{FermiShift}}$ (eV)	U (V vs SHE)	E (eV)
-2.00	-440.77	-5.13	0.23	0.30	-451.03
-1.50	-443.30	-4.96	0.23	0.13	-450.74
-1.00	-445.76	-4.84	0.23	0.01	-450.60
-0.50	-448.17	-4.73	0.23	-0.10	-450.53
0.00	-450.53	-4.52	0.23	-0.31	-450.53
0.50	-452.74	-4.32	0.23	-0.51	-450.58
1.00	-454.89	-4.18	0.23	-0.65	-450.70
1.50	-456.96	-4.04	0.23	-0.79	-450.90
2.00	-458.96	-3.89	0.23	-0.94	-451.18

Table S21. Δq , E_{VASP} , E_f , $E_{\text{FermiShift}}$, corresponding U and potential-dependent electrochemical energy E for O*Au@C₁₅N₆OS₂H₅. And the fitted $E-U$ relation is $E = -1.57U^2 - 0.67U - 445.35$, $R^2 = 0.99$.

Δq (e)	E_{VASP} (eV)	E_f (eV)	$E_{\text{FermiShift}}$ (eV)	U (V vs SHE)	E (eV)
-2.00	-435.43	-5.20	0.23	0.37	-445.83
-1.50	-438.00	-5.03	0.23	0.20	-445.54
-1.00	-440.49	-4.90	0.23	0.07	-445.39
-0.50	-442.93	-4.78	0.23	-0.05	-445.32
0.00	-445.31	-4.61	0.23	-0.22	-445.31
1.00	-449.74	-4.25	0.23	-0.58	-445.49
1.50	-451.84	-4.11	0.23	-0.72	-445.67
2.00	-453.88	-3.96	0.23	-0.87	-445.96

Table S22. Δq , E_{VASP} , E_f , $E_{\text{FermiShift}}$, corresponding U and potential-dependent electrochemical energy E for OOH*Au@C₁₅N₆OS₂H₅. And the fitted $E-U$ relation is $E = -1.94U^2 - 1.02U - 454.81$, $R^2 = 0.96$.

Δq (e)	E_{VASP} (eV)	E_f (eV)	$E_{\text{FermiShift}}$ (eV)	U (V vs SHE)	E (eV)
-2.00	-444.99	-5.09	0.23	0.25	-455.17
-1.50	-447.51	-4.94	0.23	0.11	-454.93
-1.00	-449.99	-4.82	0.23	-0.02	-454.80
-0.50	-452.39	-4.68	0.23	-0.16	-454.73
0.00	-454.73	-4.51	0.23	-0.33	-454.73
0.50	-456.95	-4.32	0.23	-0.51	-454.79
1.00	-459.09	-4.18	0.23	-0.65	-454.91
1.50	-461.18	-4.04	0.23	-0.79	-455.12
2.00	-463.44	-3.92	0.23	-0.91	-455.60

Table S23. Δq , E_{VASP} , E_f , $E_{\text{FermiShift}}$, corresponding U and potential-dependent electrochemical energy E for Cu@C₁₅N₆SO₂H₅. And the fitted $E-U$ relation is $E = -1.31U^2 - 1.84U - 448.44$, $R^2 = 0.99$.

Δq (e)	E_{VASP} (eV)	E_f (eV)	$E_{\text{FermiShift}}$ (eV)	U (V vs SHE)	E (eV)
-2.00	-438.83	-4.77	0.21	-0.04	-448.38
-1.50	-441.20	-4.62	0.21	-0.19	-448.13
-1.00	-443.48	-4.46	0.21	-0.35	-447.95
-0.50	-445.69	-4.29	0.21	-0.52	-447.84
0.00	-447.81	-4.09	0.21	-0.72	-447.81
0.50	-449.81	-3.88	0.21	-0.93	-447.87
1.00	-451.72	-3.69	0.21	-1.12	-448.03
1.50	-453.55	-3.49	0.21	-1.33	-448.31
2.00	-455.26	-3.30	0.21	-1.52	-448.67

Table S24. Δq , E_{VASP} , E_f , $E_{\text{FermiShift}}$, corresponding U and potential-dependent electrochemical energy E for OH*Cu@C₁₅N₆SO₂H₅. And the fitted $E-U$ relation is $E = -1.44U^2 - 1.47U - 457.92$, $R^2 = 0.99$.

Δq (e)	E_{VASP} (eV)	E_f (eV)	$E_{\text{FermiShift}}$ (eV)	U (V vs SHE)	E (eV)
-2.00	-448.25	-4.94	0.22	0.12	-458.12
-1.50	-450.69	-4.77	0.22	-0.05	-457.85
-1.00	-453.06	-4.62	0.22	-0.20	-457.68
-0.50	-455.34	-4.46	0.22	-0.36	-457.57
0.00	-457.55	-4.28	0.22	-0.53	-457.55
0.50	-459.66	-4.11	0.22	-0.71	-457.61
1.00	-461.69	-3.93	0.22	-0.89	-457.76
1.50	-463.62	-3.75	0.22	-1.07	-458.00
2.00	-465.46	-3.56	0.22	-1.25	-458.34

Table S25. Δq , E_{VASP} , E_f , $E_{\text{FermiShift}}$, corresponding U and potential-dependent electrochemical energy E for O*Cu@C₁₅N₆SO₂H₅. And the fitted E - U relation is $E = -1.44U^2 - 1.41U - 452.33$, $R^2 = 0.99$

Δq (e)	E_{VASP} (eV)	E_f (eV)	$E_{\text{FermiShift}}$ (eV)	U (V vs SHE)	E (eV)
-2.00	-442.66	-4.95	0.22	0.14	-452.56
-1.50	-445.11	-4.79	0.22	-0.03	-452.29
-1.00	-447.47	-4.64	0.22	-0.17	-452.11
-0.50	-449.77	-4.48	0.22	-0.33	-452.01
0.00	-451.98	-4.31	0.22	-0.51	-451.98
0.50	-454.11	-4.14	0.22	-0.68	-452.04
1.00	-456.19	-3.93	0.22	-0.89	-452.26
1.50	-458.06	-3.82	0.22	-1.00	-452.33
2.00	-459.94	-3.65	0.22	-1.17	-452.64

Table S26. Δq , E_{VASP} , E_f , $E_{\text{FermiShift}}$, corresponding U and potential-dependent electrochemical energy E for OOH*Cu@C₁₅N₆SO₂H₅. And the fitted E - U relation is $E = -1.55U^2 - 1.67U - 462.32$, $R^2 = 0.99$.

Δq (e)	E_{VASP} (eV)	E_f (eV)	$E_{\text{FermiShift}}$ (eV)	U (V vs SHE)	E (eV)
-2.00	-452.68	-4.86	0.22	0.03	-462.39
-1.50	-455.08	-4.71	0.22	-0.12	-462.14
-1.00	-457.42	-4.56	0.22	-0.26	-461.98
-0.50	-459.68	-4.40	0.22	-0.43	-461.88
0.00	-461.86	-4.25	0.22	-0.57	-461.86
0.50	-464.00	-4.08	0.22	-0.74	-461.96
1.00	-466.00	-3.90	0.22	-0.92	-462.10
1.50	-467.93	-3.74	0.22	-1.08	-462.32
2.00	-469.79	-3.58	0.22	-1.24	-462.63

Table S27. Δq , E_{VASP} , E_f , $E_{\text{FermiShift}}$, corresponding U and potential-dependent electrochemical energy E for $\text{Au}@\text{C}_{15}\text{N}_6\text{OSe}_2\text{H}_5$. And the fitted $E-U$ relation is $E = -1.59U^2 - 1.17U - 436.25$, $R^2 = 0.99$.

Δq (e)	E_{VASP} (eV)	E_f (eV)	$E_{\text{FermiShift}}$ (eV)	U (V vs SHE)	E (eV)
-2.00	-426.43	-5.06	0.26	0.20	-436.55
-1.50	-428.95	-4.93	0.26	0.08	-436.35
-1.00	-431.40	-4.78	0.26	-0.08	-436.18
-0.50	-433.75	-4.59	0.26	-0.27	-436.05
0.00	-436.03	-4.45	0.26	-0.41	-436.03
0.50	-438.23	-4.31	0.26	-0.55	-436.08
1.00	-440.37	-4.17	0.26	-0.68	-436.20
1.50	-442.44	-4.00	0.26	-0.86	-436.44
2.00	-444.40	-3.75	0.26	-1.11	-436.90

Table S28. Δq , E_{VASP} , E_f , $E_{\text{FermiShift}}$, corresponding U and potential-dependent electrochemical energy E for $\text{OH}^*\text{Au}@\text{C}_{15}\text{N}_6\text{OSe}_2\text{H}_5$. And the fitted $E-U$ relation is $E = -1.62U^2 - 0.67U - 447.13$, $R^2 = 0.99$.

Δq (e)	E_{VASP} (eV)	E_f (eV)	$E_{\text{FermiShift}}$ (eV)	U (V vs SHE)	E (eV)
-2.00	-448.25	-4.94	0.22	0.12	-458.12
-1.50	-450.69	-4.77	0.22	-0.05	-457.85
-1.00	-453.06	-4.62	0.22	-0.20	-457.68
-0.50	-455.34	-4.46	0.22	-0.36	-457.57
0.00	-457.55	-4.28	0.22	-0.53	-457.55
0.50	-459.66	-4.11	0.22	-0.71	-457.61
1.00	-461.69	-3.93	0.22	-0.89	-457.76
1.50	-463.62	-3.75	0.22	-1.07	-458.00
2.00	-465.46	-3.56	0.22	-1.25	-458.34

Table S29. Δq , E_{VASP} , E_f , $E_{\text{FermiShift}}$, corresponding U and potential-dependent electrochemical energy E for $\text{O}^*\text{Au@C}_{15}\text{N}_6\text{OSe}_2\text{H}_5$. And the fitted $E-U$ relation is $E = -1.64U^2 - 0.58U - 441.54$, $R^2 = 0.99$.

Δq (e)	E_{VASP} (eV)	E_f (eV)	$E_{\text{FermiShift}}$ (eV)	U (V vs SHE)	E (eV)
-2.00	-442.66	-4.95	0.22	0.14	-452.56
-1.50	-445.11	-4.79	0.22	-0.03	-452.29
-1.00	-447.47	-4.64	0.22	-0.17	-452.11
-0.50	-449.77	-4.48	0.22	-0.33	-452.01
0.00	-451.98	-4.31	0.22	-0.51	-451.98
0.50	-454.11	-4.14	0.22	-0.68	-452.04
1.00	-456.19	-3.93	0.22	-0.89	-452.26
1.50	-458.06	-3.82	0.22	-1.00	-452.33
2.00	-459.94	-3.65	0.22	-1.17	-452.64

Table S30. Δq , E_{VASP} , E_f , $E_{\text{FermiShift}}$, corresponding U and potential-dependent electrochemical energy E for $\text{OOH}^*\text{Au@C}_{15}\text{N}_6\text{OSe}_2\text{H}_5$. And the fitted $E-U$ relation is $E = -2.22U^2 - 1.03U - 451.02$, $R^2 = 0.99$.

Δq (e)	E_{VASP} (eV)	E_f (eV)	$E_{\text{FermiShift}}$ (eV)	U (V vs SHE)	E (eV)
-2.00	-441.15	-5.10	0.27	0.23	-451.34
-1.50	-443.70	-4.98	0.27	0.12	-451.17
-1.00	-446.18	-4.87	0.27	0.00	-451.04
-0.50	-448.58	-4.77	0.27	-0.10	-450.97
0.00	-450.96	-4.57	0.27	-0.29	-450.96
0.50	-453.22	-4.41	0.27	-0.46	-451.02
1.00	-455.41	-4.28	0.27	-0.59	-451.13
1.50	-457.55	-4.14	0.27	-0.73	-451.35
2.00	-459.88	-4.02	0.27	-0.84	-451.83

References

1. Y. Wang, M. Wang, Z. Lu, D. Ma and Y. Jia, Enabling multifunctional electrocatalysts by modifying the basal plane of unifunctional 1T'-MoS₂ with anchored transition metal single atoms, *Nanoscale*, 2021, **13**, 13390-13400.
2. X. Bai, S. Lu, P. Song, Z. Jia, Z. Gao, T. Peng, Z. Wang, Q. Jiang, H. Cui, W. Tian, R. Feng, Z. Liang, Q. Kang and H. Yuan, Heterojunction of MXenes and MN₄-graphene: Machine learning to accelerate the design of bifunctional oxygen electrocatalysts, *J. Colloid Interface Sci.*, 2024, **664**, 716-725.
3. J. H. Friedman, Stochastic gradient boosting, *Comput. Stat. Data Anal.*, 2002, **38**, 367-378.
4. J. H. Friedman, Greedy function approximation: A gradient boosting machine, *Ann. Stat.*, 2001, **29**, 1189-1232.
5. J. Quiñonero-Candela and C. E. Rasmussen, A Unifying View of Sparse Approximate Gaussian Process Regression, *J. Mach. Learn. Res.*, 2005, **6**, 1939–1959.
6. A. Seko, T. Maekawa, K. Tsuda and I. Tanaka, Machine learning with systematic density-functional theory calculations: Application to melting temperatures of single- and binary-component solids, *Phys. Rev. B*, 2014, **89**, 054303.